Check for updates

Human abdominal subcutaneous-derived active beige adipocytes carrying *FTO* rs1421085 obesity-risk alleles exert lower thermogenic capacity

Attila Vámos[1,2†], Rini Arianti[1,3†], Boglárka Ágnes Vinnai[1,2], Rahaf Alrifai[1,2], Abhirup Shaw[1], Szilárd Póliska[4], Andrea Guba[2,5], Éva Csősz[5], István Csomós[6], Gábor Mocsár[6], Cecilia Lányi[7], Zoltán Balajthy[1], László Fésüs[1] and Endre Kristóf[1*]

[1]Laboratory of Cell Biochemistry, Department of Biochemistry and Molecular Biology, Faculty of Medicine, University of Debrecen, Debrecen, Hungary, [2]Doctoral School of Molecular Cell and Immune Biology, University of Debrecen, Debrecen, Hungary, [3]Universitas Muhammadiyah Bangka Belitung, Pangkalanbaru, Indonesia, [4]Genomic Medicine and Bioinformatics Core Facility, Department of Biochemistry and Molecular Biology, Faculty of Medicine, University of Debrecen, Debrecen, Hungary, [5]Proteomics Core Facility, Department of Biochemistry and Molecular Biology, Faculty of Medicine, University of Debrecen, Debrecen, Hungary, [6]Department of Biophysics and Cell Biology, Faculty of Medicine, University of Debrecen, Debrecen, Hungary, [7]Laser Clinic, Budapest, Hungary

Introduction: White adipocytes store lipids, have a large lipid droplet and few mitochondria. Brown and beige adipocytes, which produce heat, are characterized by high expression of uncoupling protein (UCP) 1, multilocular lipid droplets, and large amounts of mitochondria. The rs1421085 T-to-C single-nucleotide polymorphism (SNP) of the human *FTO* gene interrupts a conserved motif for ARID5B repressor, resulting in adipocyte type shift from beige to white.

Methods: We obtained abdominal subcutaneous adipose tissue from donors carrying *FTO* rs1421085 TT (risk-free) or CC (obesity-risk) genotypes, isolated and differentiated their preadipocytes into beige adipocytes (driven by the PPARγ agonist rosiglitazone for 14 days), and activated them with dibutyryl-cAMP for 4 hours. Then, either the same culture conditions were applied for additional 14 days (active beige adipocytes) or it was replaced by a white differentiation medium (inactive beige adipocytes). White adipocytes were differentiated by their medium for 28 days.

Results and Discussion: RNA-sequencing was performed to investigate the gene expression pattern of adipocytes carrying different *FTO* alleles and found that active beige adipocytes had higher brown adipocyte content and browning capacity compared to white or inactive beige ones when the cells were obtained from risk-free TT but not from obesity-risk CC genotype carriers. Active beige adipocytes carrying *FTO* CC had lower thermogenic gene (e.g., *UCP1, PM20D1, CIDEA*) expression and thermogenesis measured by proton leak respiration as compared to TT carriers. In addition, active beige adipocytes with CC alleles exerted lower expression of ASC-1 neutral amino acid transporter (encoded by *SLC7A10*) and less consumption of Ala, Ser, Cys, and Gly as compared to risk-free carriers. We did not observe any influence of the *FTO* rs1421085 SNP

on white and inactive beige adipocytes highlighting its exclusive and critical effect when adipocytes were activated for thermogenesis.

1 Introduction

In the last few decades, the prevalence of obesity dramatically increased across the world. Chronic obesity can lead to various cancers, type 2 diabetes, and cardiovascular disease. Therefore, obesity has been identified as one of the globally leading causes of mortality and disability, and is responsible for 10%–13% of deaths in different regions worldwide (Frühbeck et al., 2013). Imbalance of energy homeostasis, when energy intake is significantly greater than energy expenditure, has been identified as the main pathophysiological cause of obesity (Heymsfield and Wadden, 2017). However, obesity is a multifactorial disease which can be the result of factors including social, lifestyle, behavioral networks, and genetic background of the individuals (Christakis and Fowler, 2007; Frühbeck et al., 2018; Lin and Li, 2021).

In rodents, adipocytes are classified into three types. The energy storing white adipocytes have one large unilocular lipid droplet and low mitochondrial density. The brown adipocytes located in the brown adipose tissue (BAT) are active thermogenic cells with high mitochondrial abundance, fragmentation, and uncoupling protein (UCP) 1 expression, as well as numerous small lipid droplet content in the cytoplasm. The "brown-like-in-white" (brite) or beige cells have cold-inducible thermogenic potential and multilocular lipid droplets (Sanchez-Gurmaches et al., 2016). Beige adipocytes are interspersed in the white adipose tissue (WAT). In basal state, their gene expression pattern is similar to the white adipocytes, but upon extended stimuli (cold exposure, β-adrenergic stimulation, peroxisome proliferator-activated receptor (PPAR)-γ activation) they exhibit a brown-like phenotype acquired in a process called browning (Petrovic et al., 2010; Wu et al., 2012). Inguinal WAT has been discovered as a natural beige adipocyte depot, in which the adipocytes possess multilocular morphology and thermogenic gene expression profile in response to thermogenic cues (Chan et al., 2019).

In humans, BAT was primarily regarded as a tissue which is only present in infants and located at anatomical sites that are difficult to reach (Heaton, 1972). Several studies using positron emission tomography (PET) provided evidence that adults have significant amounts of BAT, most commonly the cervical-supraclavicular depot was marked by high labeled glucose uptake especially after cold exposure (Cypess et al., 2009; Virtanen et al., 2009). Using an elegant approach of the PET-Computed Tomography (CT) method, brownable adipose tissue could be found interspersed in several areas, such as cervical, supraclavicular, axillary, mediastinal, paraspinal, and abdominal (Leitner et al., 2017). However, unlike in rodents, the molecular characteristics of human BAT remain elusive. Several studies reported that human BAT isolated from cervical-supraclavicular depots (Cypess et al., 2013) and primary adipocytes derived from fetal interscapular adipose tissue (Seiler et al., 2015) possess classical brown adipocyte characteristics marked by high expression of zinc finger protein-1 (ZIC1), whereas other studies using clonally derived human brown adipocytes isolated from supraclavicular depot reported the existence of a population of UCP1-

positive cells displaying beige adipocyte features (Shinoda et al., 2015). Another study using total RNA isolated from fat biopsies from various anatomical locations, including subcutaneous (SC) supraclavicular, posterior mediastinal, retroperitoneal, intra-abdominal, or mesenteric depots reported that beige-selective markers, such as *HOXC8*, *HOXC9*, and *CITED1* were highly expressed in human thermogenic adipose tissue, whereas classical BAT markers were not detectable (Sharp et al., 2012).

The activation of UCP1 to generate heat by brown/beige adipocytes drives a higher uptake of fuels, such as glucose and fatty acids, to sustain the metabolic substrates for tricarboxylic acid (TCA) cycle and generate NADH and FADH$_2$ that subsequently enter the electron transport chain. Active brown/beige adipocytes also take up large amounts of TCA cycle intermediates, e.g., succinate, to enhance their proton leak respiration (Mills et al., 2018). A recent study reported that the labeled glucose consumed by murine BAT during cold exposure is converted to pyruvate, which is further oxidized to acetyl-CoA catalyzed by pyruvate dehydrogenase (Panic et al., 2020). In addition to glucose and fatty acids, active brown/beige adipocytes also catabolize branched-chain amino acids to fulfill the high demand of energy (Yoneshiro et al., 2019). Our previous study also underlined the importance of alanine-serine-cysteine transporter 1 (ASC-1)-mediated consumption of serine, cysteine, and glycine for efficient thermogenic response upon adrenergic stimulation in deep neck derived adipocytes (Arianti et al., 2021). The capability of active brown/beige adipocytes as metabolic sink may contribute to the clearance of blood glucose and lipids, which indirectly improves glucose tolerance and insulin sensitivity (Cheng et al., 2021). High rate of metabolic substrate utilization by active brown/beige adipocytes enhances the energy expenditure, therefore it may promote weight loss and become a potential pharmaceutical target to treat obesity and related metabolic diseases.

Recent publications reported the involvement of autophagy in the downregulation of beige adipocyte thermogenesis. In rodents, parkin-dependent selective mitochondrial clearance (mitophagy) drives the generation of inactive–morphologically white, but reactivation capable–masked beige adipocytes (Altshuler-Keylin et al., 2016). In human abdominal SC adipocytes, both parkin-dependent and parkin-independent mitophagy related genes were upregulated upon *ex vivo* beige to white transition (Vámos et al., 2022). In contrast, in differentiated human primary SC and Simpson–Golabi–Behmel syndrome (SGBS) adipocytes, cAMP-induced thermogenic activation downregulated mitophagy blocking beige to white transition (Szatmári-Tóth et al., 2020). Preventing entry into this conversion might be a potential way to maintain elevated thermogenesis for combatting obesity.

Individual susceptibility to obesity is determined by interactions between genetic background and behavior. Genome-wide association studies identified the strong association between obesity and the Fat mass and obesity-associated (*FTO*) gene

(Wang et al., 2011; Dina et al., 2007; Frayling et al., 2007; Scuteri et al., 2007). Among several identified single-nucleotide polymorphisms (SNPs) of *FTO*, an intronic rs1421085 T-to-C SNP has recently attracted attention. Studies in European and Japanese populations reported that the presence of the obesity-risk C allele increased the susceptibility for obesity, elevated fat mass and food intake (Wheeler et al., 2013; Felix et al., 2016; Imamura et al., 2016; Tanaka et al., 2013). Claussnitzer et al. (2015) elucidated the molecular background for the association between *FTO* rs1421085 SNP and increased fat storage. In the presence of the risk-free allele (T), the AT-Rich Interaction Domain 5B (ARID5B) repressor protein can bind to the enhancer region of Iroquois Homeobox (IRX) 3 and 5, therefore the expression of IRX3 and 5 is suppressed (Claussnitzer et al., 2015). When the obesity-risk allele is present, the conserved motif for ARID5B repressor is disrupted resulting in elevated expression of IRX3 and 5. As the consequence, the differentiation program is shifted from energy dissipation by beige adipocytes to lipid storage into white adipocytes (Claussnitzer et al., 2015; Herman and Rosen, 2015). IRX5$^{-/-}$ mice possessed reduced fat mass and did not develop obesity when fed on a high-fat diet. In addition, *IRX5* silencing increased the mitochondrial respiration in isolated mouse adipocytes (Bjune et al., 2005). IRX3$^{-/-}$ ME3 murine embryonic fibroblast line failed to differentiate to beige adipocytes, however, increased their capacity for chondrogenesis (Bjune et al., 2020). On the other hand, it was also reported that IRX3 promotes the browning of white adipocytes as it can directly bind to the promoter of *UCP1* (Zou et al., 2017).

In this study, we employed transcriptomic and metabolomic data to investigate the effect of *FTO* rs1421085 SNP on the thermogenic capacity of three types of adipocytes: white, active and inactive beige, which were derived from human adipose-derived stromal cells (hASCs) isolated from abdominal SC fat of donors carrying *FTO* risk-free (TT) or obesity-risk (CC) genotypes (4 individuals of each genotype). RNA-sequencing (RNA-seq) analysis was performed to screen the global transcriptomic profiles of the differentiated adipocytes and we found that active beige adipocytes carrying risk-free alleles had higher brown adipocyte content, browning capacity, mitochondrial complex I, II, and IV subunit amount, proton leak respiration, extracellular acidification, expression of thermogenic markers (*UCP1*, *PM20D1*, *CITED1*, *CIDEA*, *CKMT1*, and *CKMT2*), and ASC-1-mediated amino acid consumption, as compared to white or inactive beige adipocytes carrying the same genotypes. Intriguingly, we found that active beige adipocytes carrying *FTO* obesity-risk genotypes have less distinguishable characteristics as compared to white or inactive beige adipocytes. Our findings underline the critical effect of *FTO* rs1421085 SNP in human abdominal SC adipocytes when they are activated for thermogenesis.

2 Materials and methods

2.1 Materials

All chemicals and reagents were obtained from Sigma-Aldrich (Munich, Germany) unless stated otherwise.

2.2 Ethical statement and obtained hASCs

The human SC abdominal adipose tissue collection was approved by the Medical Research Council of Hungary (20571-2/2017/EKU) followed by the EU Member States' Directive 2004/23/EC on presumed consent practice for tissue collection. All experiments were implemented in accordance with the Helsinki Declaration. All participants were informed about the experiments and written informed consent was obtained from them. hASCs were obtained and isolated from stromal vascular fractions (SVFs) of human SC abdominal adipose tissue of healthy donors undergoing plastic surgery, as previously described (Kristóf et al., 2019; Szatmári-Tóth et al., 2020). Briefly, the tissue samples were immediately transported to the laboratory following plastic surgery. Adipose tissue specimens were dissected from fibrous material and blood vessels, minced into small pieces and digested in phosphate buffered saline (PBS) with 120 U/mL collagenase for 120 min in a 37°C water bath with gentle agitation. The completely disaggregated tissue was filtered (pore size 140 μm) to remove any remaining tissue. The cell suspension was centrifuged for 10 min at 1,300 rpm and the pellet of SVF was suspended and maintained. Floating cells were washed away with PBS after 3 days of isolation and the remaining cells were cultured as described in 2.3. Data of the donors included in the study are listed in Supplementary Table S1.

2.3 Maintenance and differentiation of hASCs

hASCs were seeded in 6-well plates and cultured in Dulbecco's Modified Eagle's Medium/Nutrient F-12 Ham (DMEM-F12) medium containing 17 μM pantothenic acid, 33 μM biotin, 100 U/mL penicillin/streptomycin, and 10% fetal bovine serum (Thermo Fisher Scientific, Waltham, MA, United States) at 37°C in 5% CO_2 until they reach complete confluence. The absence of *mycoplasma* was verified by polymerase chain reaction (PCR) analysis (PCR *Mycoplasma* Test Kit I/C, PromoKine, PromoCell, Heidelberg, Germany).

White adipogenic differentiation was induced for 3 days with serum-free DMEM-F12 medium supplemented with 17 μM pantothenic acid, 33 μM biotin, 100 U/mL penicillin/streptomycin, 100 nM cortisol, 10 μg/mL human apo-transferrin, 200 pM triiodothyronine, 20 nM human insulin, 2 μM rosiglitazone (Cayman Chemicals, Ann Arbor, MI, United States), 25 nM dexamethasone, and 500 μM 3-isobutyl-l-methylxantine. After the third day, rosiglitazone, dexamethasone, and 3-isobutyl-l-methylxantine were removed from the medium during the remaining 25 days of the differentiation. The medium was exchanged in every third day.

The active beige differentiation was induced for 3 days with serum-free DMEM-F12 medium supplemented with 17 μM pantothenic acid, 33 μM biotin, 100 U/mL penicillin/streptomycin, 10 μg/mL human apo-transferrin, 200 pM triiodothyronine, 20 nM human insulin, 2 μM rosiglitazone, 25 nM dexamethasone, and 500 μM 3-isobutyl-l-methylxantine. After the third day, dexamethasone and 3-isobutyl-l-methylxantine were removed and 500 nM rosigliazone was added to the medium for the remaining 25 days of differentiation. On the 14th day, a 4 h long 500 μM dibutyryl-cAMP treatment was carried out to mimic the *in vivo* cold-induced thermogenesis (Szatmári-Tóth et al., 2020). After the treatment, the aforementioned beige differentiation medium was applied until the end of the differentiation.

The inactive beige differentiation was induced in the first 14 days as in the case of the active beige adipocytes, but after the dibutyryl-

cAMP treatment, the medium was replaced to the white cocktail without rosiglitazone, dexamethasone, and 3-isobutyl-l-methylxanthine for additional 14 days.

2.4 RNA isolation, reverse-transcription PCR (RT-PCR), quantitative PCR (qPCR), and RNA-Seq analysis

Adipocytes were collected in TRIzol reagent (Thermo Fisher Scientific), followed by manual RNA isolation by chloroform extraction and isopropanol precipitation. The RNA quality was evaluated by Nanodrop (Thermo Fisher Scientific). cDNA generation was carried out by TaqMan reverse transcription reagent kit (Thermo Fisher Scientific) and followed by qPCR analysis (Szatmári-Tóth et al., 2020; Shaw et al., 2021). Gene expressions were normalized to the geometric mean of β-actin (*ACTB*) and *GAPDH*. All TaqMan assays are listed in Supplementary Table S2.

Total RNA sample quality was checked on Agilent BioAnalyzer using Eukaryotic Total RNA Nano Kit according to the Manufacturer's protocol. Samples with RNA integrity number (RIN) value >7 were accepted for the library preparation process. RNA-Seq libraries were prepared from total RNA using MGIEasy RNA Library Prep Set V3.0 (MGI, Shenzhen, China) according to the manufacturer's protocol. Briefly, poly-A RNAs were captured by oligo-dT conjugated magnetic beads then the mRNAs were eluted and fragmented at 94°C. First-strand cDNA was generated by random priming reverse transcription, then in the second strand synthesis step, double-stranded cDNA was generated. After repairing ends, A-tailing and adapter ligation steps, adapter-ligated fragments were amplified in enrichment PCR and finally sequencing libraries were generated. In the next step double-stranded libraries were denatured and single strand circularization was performed, after enzymatic digestion step circularized single-stranded library was generated for DNA nano ball (DNB) generation. After making DNB step, single-end 100 cycles sequencing run was executed on MGI DNBSEQ G400 instrument. After sequencing, the reads were aligned to the GRCh38 reference genome (with EnsEMBL 95 annotation) using STAR aligner (version 2.7.0a). FeatureCounts was used to quantify our reads to genes. Significantly differentially expressed genes (DEGs) were defined based on adjusted p values <0.05 and log2 fold change threshold >0.85. Heatmap was generated by using GraphPad 8.0 Software and interactome map was constructed by using Gephi 0.9 based on interaction from STRING (https://string-db.org/). Pathway analysis was performed by subjecting the list of DEGs to STRING and overrepresented KEGG pathways were selected based on the false discovery rate (FDR) < 0.05. Brown adipocyte content and browning capacity was estimated by BATLAS and ProFAT webtools, respectively, by subjecting the transcriptomic data of both groups of markers (Perdikari et al., 2018; Cheng et al., 2018).

2.5 *FTO* allele genotyping

DNA isolation was performed as previously described (Klusóczki et al., 2019). Rs1421085 SNP was genotyped by qPCR using TaqMan SNP Genotyping assay (Thermo Fisher Scientific, 4351379) according to the Manufacturer's instructions.

2.6 Antibodies and immunoblotting

The separation of investigated proteins was performed by SDS-PAGE, followed by transfer to a PVDF membrane, which was blocked by 5% skimmed milk solution (Szatmári-Tóth et al., 2020; Shaw et al., 2021). The primary antibodies were utilized in the following dilutions: anti-β-actin (1:5000, A2066), anti-UCP1 (1:750, R&D Systems, Minneapolis, MN, United States, MAB6158), anti-OXPHOS (1:1,000, Abcam, Cambridge, MA, United States, ab110411), anti-SLC7A10 (1:500, Abnova, Taipei City, Taiwan, H00056301-B01P), anti-PGC1α (1:1,000, Novus Biologicals, Centennial, CO, United States, NBP1-04676) anti-GPT2 (1:2000, Thermo Fisher Scientific, PA5-62426), and anti-SHMT1 (1:2000, Thermo Fisher Scientific, PA5-88581). The following species corresponding secondary antibodies were used: HRP-conjugated goat anti-mouse (1:5000, Advansta, San Jose, CA, United States, R-05071-500) or anti-rabbit (1:5000, Advansta, R-05072-500) IgG. The expression of the visualized immunoreactive proteins were quantified by densitometry using the FIJI ImageJ software (National Institutes of Health (NIH), Bethesda, MD, United States) as previously described (Szatmári-Tóth et al., 2020).

2.7 Immunofluorescent staining

hASCs were seeded and differentiated on Ibidi eight-well µ-slides as described in Section 2.3. Cells were washed once with PBS and fixed by 4% paraformaldehyde, followed by permeabilization with 0.1% saponin and blocking with 5% skimmed milk. Primary antibody incubations were kept overnight with anti-TOM20 (1:75, WH0009804M1) and anti-LC3 (1:200, Novus Biologicals, NB100-2220). Secondary antibody incubation was for 3 h with Alexa Fluor 647 goat anti-mouse IgG (1:1,000, Thermo Fisher Scientific, A21236) and Alexa Fluor 488 goat anti-rabbit IgG (1:1,000, Thermo Fisher Scientific, A11034). Propidium iodide (PI, 1.5 µg/mL, 1 h) was used for nuclei labeling. Images were obtained with an Olympus FluoView 1,000 (Olympus Scientific Solutions, Tokyo, Japan) confocal microscope and FluoView10-ASW (Olympus Scientific Solutions) software version 3.0, as previously described (Szatmári-Tóth et al., 2020; Vámos et al., 2022). LC3 and TOM20 immunostaining images were converted to binary form, followed by processing with FIJI. The LC3 punctae count was determined by size (pixel^2) 50–infinity AU with circularity 0–1 AU. Fragmented mitochondria were analyzed from the binary TOM20 immunostaining images with size (pixel^2) 0–100 AU and circularity 0–1 AU. The optimum size values for the LC3 punctae and fragmented mitochondria were determined based on an analysis of all immunostaining images and manual verification of the counting accuracy by checking the outlines of counts. Both LC3 punctae and fragmented mitochondria content were normalized to per nucleus for individual images. Co-localization of LC3 and TOM20 was evaluated by calculation of the Pearson correlation coefficient (PCC) (Szatmári-Tóth et al., 2020; Vámos et al., 2022). 30 cells per three donors were recorded and analyzed.

2.8 Quantification of amino acid fluxes of adipocytes

Supernatants of the cells were collected at the end of the differentiation process and examined as previously described (Guba et al., 2022; Nokhoijav et al., 2022). Briefly, the media were filtered using a 3 kDa filter (Pall Corporation, Port Washington, NY, United States) and 10 μL of this filtrate was derivatized with AccQ Tag Ultra Derivatization Kit (Waters, Milford, MA, United States). Chromatographic separation was executed on H-class UPLC (Waters) using AccQ Tag Ultra Column (2.1 × 100 mm), AccQ Tag Eluent A and B, and gradient was ensured by the AccQ Tag Ultra Chemistry Kit (Waters). Amino acid (both L and D enantiomers) derivatives were detected at 260 nm in the PDA detector of the UPLC. Detection of the amino acid concentrations were calculated by Empower software (Waters) using a 7-point calibration curve. Flux of amino acids into or from adipocytes was calculated by comparing concentration differences measured in the conditioned media, which was administered to the cells at day 25 and collected at the end point of 28 days differentiation, and the unconditioned medium. The concentration of amino acids was normalized to the number of cells as described previously (Arianti et al., 2021).

2.9 Determination of real-time cellular oxygen consumption (OCR) and extracellular acidification rate (ECAR)

Cells were seeded and differentiated on XF96 assay plates (Seahorse Biosciences, North Billerica, MA, United States) to white, active beige, or inactive beige using the protocols as described in Section 2.3. The OCR and ECAR were measured with XF96 oximeter (Seahorse Biosciences). Dibutyryl-cAMP stimulated OCR and ECAR, etomoxir-resistant (ETO-R) OCR, and stimulated proton leak OCR were quantified using previously utilized protocols (Kristóf et al., 2015; Arianti et al., 2021; Nagy et al., 2022). 10 μM antimycin A was used for baseline collection (measuring non-mitochondrial respiration). The OCR was normalized to protein content of each well.

2.10 Statistical analysis

All results are expressed as mean ± SD. The normality of the obtained data was tested by Shapiro-Wilk test. Datasets with a normal distribution was analyzed using one-way ANOVA with a Tukey's *post hoc* test. Data was analyzed and visualized by GraphPad Prism 8 Software.

3 Results

3.1 Active beige adipocytes derived from abdominal SC exert high browning capacity

Primarily, we aimed to investigate the global gene expression patterns of the three types of differentiated SC adipocytes, white,

active, and inactive beige (see Methods for their differentiation protocol) by performing RNA-seq analysis. We found that general adipocyte markers, such as *SLC2A4*, *FABP4*, *LPL*, *ADIPOQ*, *AGPAT2*, *PLIN1*, *LEP*, and *LEPR* were not expressed differentially among the three types of adipocytes (Figure 1A) suggesting that their differentiation rate was similar. The thermogenic markers, such as *UCP1*, *ELOVL3*, *PGC1a*, *CIDEA*, *CITED1*, *AQP3*, *GK*, *CKMT1a/b*, and *PM20D1* had higher expression in active beige as compared to white or inactive beige adipocytes (Figure 1B). Next, we subjected our transcriptomic data from RNA-seq analysis to open source webtools to estimate brown adipocyte content by BATLAS (Perdikari et al., 2018) and browning capacity by ProFAT (Cheng et al., 2018) based on the expression levels of well-defined marker genes. We did not find significant differences in brown adipocyte content (Figure 1C), however, active beige adipocytes showed higher browning capacity score as compared to white or inactive beige ones (Figure 1D). According to our RNA-seq analysis data, we found that 211 and 147 genes had higher expression in the comparison of active beige vs. white and active beige vs. inactive beige, respectively; out of those, 100 genes were common (Figure 1E, top panel; Supplementary Tables S3, S4). Among the commonly highly expressed 100 genes, thermogenic markers, such as *GK*, *PM20D1*, *PLIN5*, *CITED1*, and *AQP3* were found (Figure 1F). Interestingly, *SLC7A10*, encoding ASC-1, which was described as an important transporter during thermogenic activation (Arianti et al., 2021; Jersin et al., 2021) was also commonly upregulated in both comparisons (Figure 1F). 248 and 226 genes had lower expression in the comparison of active beige vs. white and active beige vs. inactive beige, respectively, and 164 genes had commonly lower expression (Figure 1E, bottom panel; Supplementary Tables S3, S4). We did not find any DEGs when we compared the gene expression profile of white and inactive beige adipocytes. We also analyzed the mitophagy rate and mitochondrial morphology by co-immunostaining of microtubule-associated protein 1 light chain 3 (LC3) and translocase of outer mitochondrial membrane 20 (TOM20) [Szatmári-Tóth et al., 2020] (Figure 1G). Confocal images were used to quantify the co-localization of LC3 and TOM20 by measuring the correlation between pixel intensities of two detection channels [Szatmári-Tóth et al., 2020]. We observed lower LC3 punctae counts per cell (Figure 1H) and PCC values in active beige as compared to white or inactive beige adipocytes (Figure 1I). We also found that active beige adipocytes had higher amounts of fragmented mitochondria, which were shown to support uncoupled respiration and enhanced energy expenditure (Pisani et al., 2018), as compared to white or inactive beige cells (Figure 1J). Altogether, these data suggests that thermogenesis-related genes were upregulated, the mitophagy rate was lowered, and mitochondria were more fragmented when human abdominal SC adipocytes were activated for thermogenesis.

3.2 Active beige adipocytes carrying *FTO* rs1421085 obesity-risk alleles had lower brown adipocyte content and expressed lower level of genes involved in metabolic pathways

Next, we intended to investigate whether *FTO* rs1421085 SNP affected the browning capacity of human abdominal SC adipocytes,
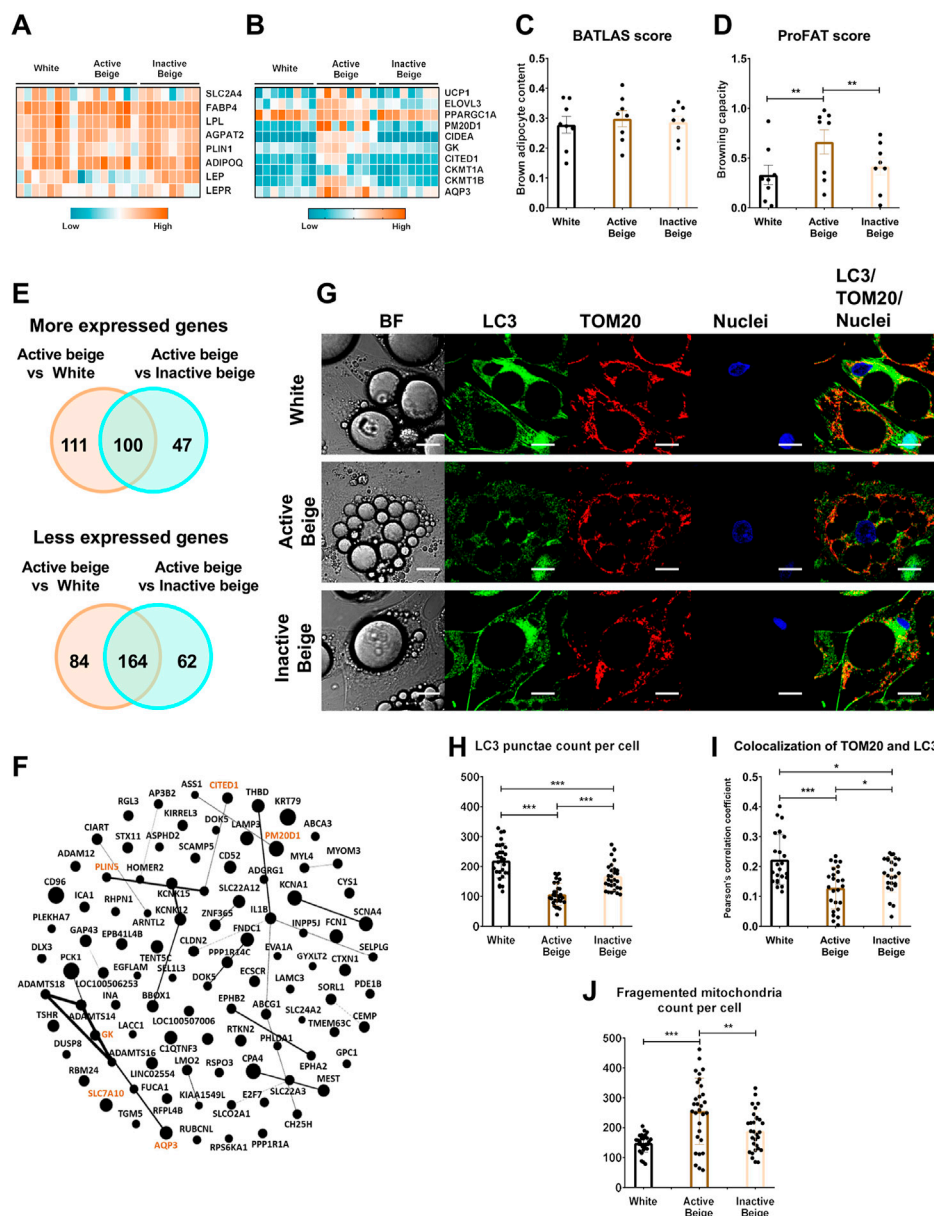
FIGURE 1
Differentially expressed genes and thermogenic capacity of human abdominal subcutaneous adipocytes. **(A)** Heatmap displaying the expression of general markers of adipocytes. **(B)** Heatmap displaying the expression of brown/beige adipocyte markers. **(C)** Brown adipocyte content quantified by BATLAS open source webtool, $n = 8$. **(D)** Browning capacity quantified by ProFAT open source webtool, $n = 8$. **(E)** Venn diagram displaying the numbers of more (top panel) and less (bottom panel) expressed genes in comparison of active beige vs. white and active beige vs. inactive beige adipocytes. **(F)** Overlapping upregulated genes between active beige vs. white and active beige vs. inactive beige in interactome map generated by Gephi. The size of the nodes correlates with fold change in the expression values. Gene names marked in brown are known thermogenic markers. **(G)** Representative confocal microscopy images of microtubule-associated protein 1 light chain 3 (LC3) and Translocase of outer mitochondrial membrane (TOM) 20 immunostaining of white, active beige, and inactive beige adipocytes. BF: bright field, scale bars represent 10 μm. **(H)** Quantification of LC3 punctae, $n = 30$ cells of three donors. **(I)** Co-localization of TOM20 and LC3, $n = 25$ per cells cells of three donors. **(J)** Quantification of fragmented mitochondria count per cell, $n = 30$ cells of three donors. Statistical analysis by ANOVA. $*p < 0.05$, $**p < 0.01$, and $***p < 0.001$.

which were differentiated into white, active, or inactive beige. Therefore, we genotyped the hASCs for *FTO* rs1421085 SNP by using SNP genotyping assay and obtained the allelic discrimination plot (Figure 2A). Then, we selected samples from 4 individuals with homozygous TT (risk-free) and from 4 individuals with homozygous CC (obesity-risk) genotypes for further analysis. We found that active beige adipocytes carrying *FTO* obesity-risk alleles

exerted lower brown adipocyte content estimated by BATLAS (Perdikari et al., 2018), but no effect of the allelic distribution was observed in case of white or inactive beige adipocytes (Figure 2B). We also found that the risk-free genotype carrier active beige adipocytes had higher tendency of BATLAS and significantly higher ProFAT (Cheng et al., 2018) scores as compared to white ones that carried the same TT genotype
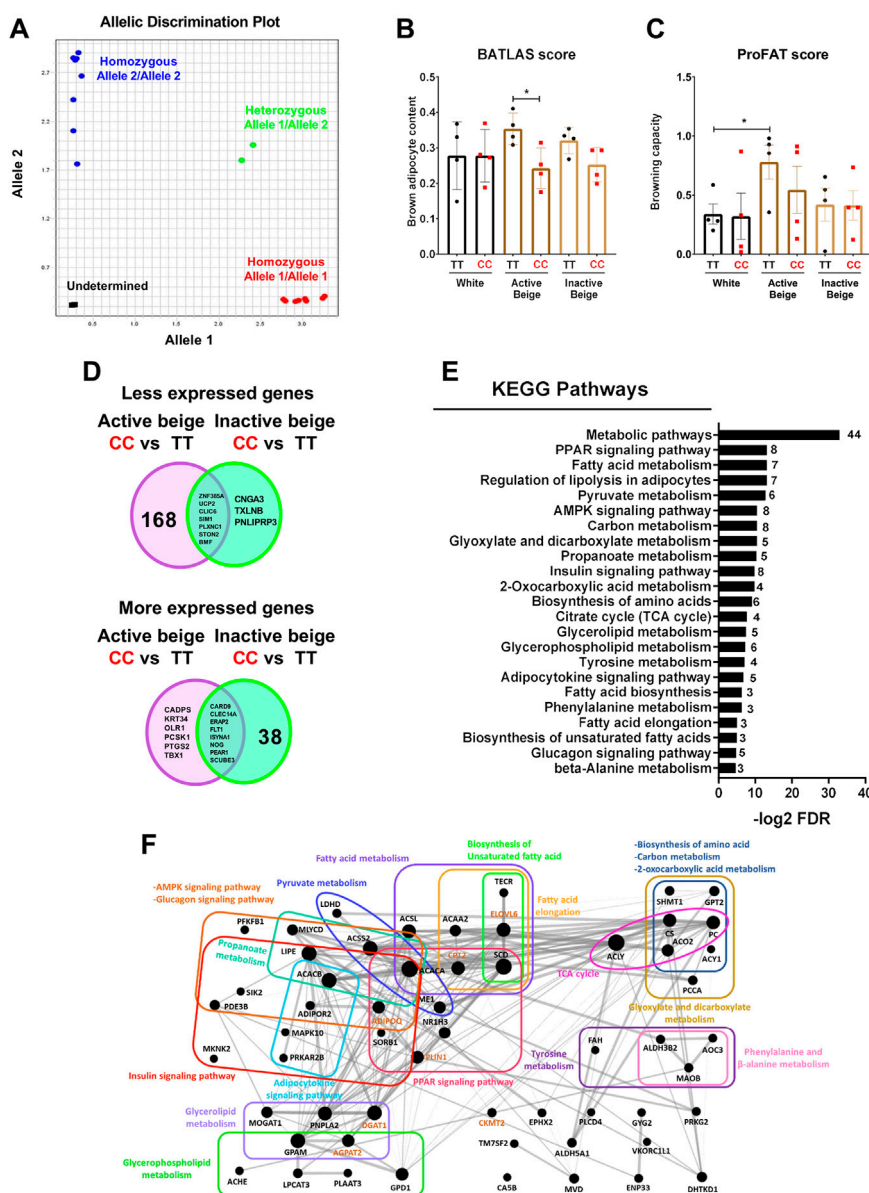
FIGURE 2
The effect of *FTO* rs1421085 SNP on the thermogenic capacity and gene expression pattern of differentiated abdominal subcutaneous (SC) adipocytes. **(A)** Allelic distribution of *FTO* rs1421085 SNP. Blue: SC progenitors with TT alleles, red: SC progenitors with CC alleles, green: heterozygous SGBS adipocytes, black: no template negative control. **(B)** Brown adipocyte content quantified by BATLAS, *n* = 4 of each genotype. **(C)** Browning capacity quantified by ProFAT, *n* = 4 of each genotype, **p* < 0.05, ***p* < 0.01, statistical analysis by ANOVA. **(D)** Venn diagram displaying the numbers of less (top panel) and more (bottom panel) expressed genes in comparison of *FTO* rs1421085 CC vs. TT in both active and inactive beige differentiated adipocytes. **(E)** Overrepresented pathways which are less expressed in active beige differentiated adipocytes carrying *FTO* CC/obesity-risk variant as compared to TT/risk-free variant. Numbers on the right side indicate the number of genes involved in the pathways. **(F)** Genes involved in less expressed pathways shown in figure **(E)** in interactome map generated by Gephi. The size of the nodes correlates with fold change of the expression values. Gene names marked in brown are known thermogenic markers.

(Figures 2B, C). Interestingly, active beige adipocytes carrying *FTO* obesity-risk genotype showed similar estimated brown adipocyte content and browning capacity as compared to white adipocytes (Figures 2B, C) suggesting that active beige differentiation could not overcome the browning inhibitory effect of the CC alleles. Active beige adipocytes with *FTO* risk-free genotype expressed the BATLAS marker genes at the highest level, whereas ones with the obesity-risk allele carriers expressed them at a level similar to

those observed in the white or inactive beige adipocytes (Supplementary Figure S1). The expression of ProFAT markers was high in risk-free carrier active beige adipocytes and showed large donor variability in the obesity-risk allele carrier ones (Supplementary Figure S2).

A total of 175 genes including thermogenic markers (*UCP2*, *CKMT2*, and *CITED1*) and 5 BATLAS markers (*PPARGC1B*, *ACO2*, *ACSF2*, *NNAT*, and *DMRT2*) were expressed less in active beige

adipocytes carrying *FTO* obesity-risk variant as compared to risk-free carriers (Figure 2D, top panel; Supplementary Table S5). Only 10 genes (7 of them were common in both comparisons) were expressed at a lower extent in CC as compared to TT carrier inactive beige adipocytes (Figure 2D, top panel; Supplementary Table S6). We found only 14 and 46 genes (8 of them were common in both comparisons) which were expressed more in active or inactive beige adipocytes, respectively, carrying the *FTO* obesity-risk as compared to the risk-free variant (Figure 2D, bottom panel; Supplementary Tables S5, S6). In white adipocytes, we did not find any DEGs which was affected by the *FTO* rs1421085 SNP. Next, we investigated the gene expression pathways affected by the *FTO* rs1421085 SNP and found that genes, which were less expressed in active beige adipocytes that carried the obesity-risk genotype, were overrepresented in several pathways, such as metabolic, PPAR signaling, lipolysis, fatty acid metabolism, or TCA cycle (Figures 2E, F). More expressed genes in active beige adipocytes with CC alleles were not significantly overrepresented in any of the pathways. We did not find any overrepresented pathway with respect to the DEGs found in inactive beige adipocytes either.

Because we observed significant effects of *FTO* rs1421085 SNP on the gene expression pattern of active beige SC adipocytes, we also compared the transcriptomic data of active beige and white or inactive beige adipocytes that carried *FTO* risk-free or obesity-risk genotypes, respectively. We found a total of 226 genes that were expressed more in active beige as compared to white adipocytes with *FTO* risk-free genotype, whereas only 54 higher expressed genes were found between the two types of differentiations in obesity-risk carriers; 25 genes were overlapping in the two comparisons (Supplementary Figure S3A; Supplementary Tables S7, S8). There were 93 and 130 genes which were expressed less in active beige as compared to white adipocytes carrying *FTO* risk-free or obesity-risk alleles, respectively. Out of those, 46 were common (Supplementary Figure S3B; Supplementary Tables S7, S8). The PPAR signaling pathway was the only one in which more expressed genes in active beige as compared to white adipocytes carrying *FTO* risk-free variant were overrepresented. The less expressed genes in active beige adipocytes as compared to white ones were overrepresented in several pathways, such as axon guidance or longevity regulating only in *FTO* obesity-risk genotype carriers (Supplementary Figure S3C). When adipocytes carried the risk-free alleles, no overrepresented pathway was found in this comparison.

We found a total of 172 genes that were expressed more in active as compared to inactive beige adipocytes carrying *FTO* risk-free variant, whereas only 18 genes were found in the same comparison with obesity-risk genotype carrier cells; nine genes were overlapping in the two comparisons (Supplementary Figure S3D; Supplementary Tables S9, S10). There were 116 and 158 genes (61 common), which were expressed less in active as compared to inactive beige adipocytes carrying *FTO* risk-free or obesity-risk alleles, respectively (Supplementary Figure S3E; Supplementary Tables S9, S10). Genes expressed in a lower extent in active beige adipocytes as compared to white ones were overrepresented in several pathways, such as AMPK signaling and TGF-beta signaling only in *FTO* obesity-risk allele carriers (Supplementary Figure S3F). When adipocytes carried the risk-free genotype, we did not find any overrepresented pathway in comparison of active with

white or inactive beige adipocytes. These results suggest that *FTO* rs1421085 SNP only affects the gene expression profile, particularly that of the thermogenesis-related genes, in active beige but not in white or inactive beige adipocytes. In addition, the applied differentiation protocols resulted in more pronounced differences in the gene expression patterns of adipocytes with *FTO* risk-free alleles which suggest their significant browning potential when thermogenic cues are constantly present.

3.3 Thermogenic marker genes were less expressed in active beige adipocytes carrying *FTO* obesity-risk alleles

Since we observed that the allelic discrimination at *FTO* rs1421085 SNP influences the expression of thermogenic and BATLAS markers, we went further to investigate the expression of thermogenic genes at mRNA and protein levels in abdominal SC adipocytes. Our results showed that the mRNA expression of *UCP1* was higher in active beige as compared to white or inactive beige adipocytes with *FTO* risk-free alleles, however, this difference was not observed in obesity-risk carriers (Figure 3A). At the protein level, we observed that active beige adipocytes expressed more UCP1 as compared to white or inactive beige adipocytes regardless the *FTO* rs1421085 genotypes, however, less UCP1 protein amount was detected in obesity-risk than in risk-free allele carrier active beige adipocytes (Figure 3B). Other thermogenic genes, such as *UCP2*, *PM20D1*, *CIDEA*, *CITED1*, *CKMT1* and *2*, *CPT2*, and *PLIN1* were also expressed higher in active beige adipocytes carrying risk-free alleles as compared to white or inactive beige adipocytes with the same TT variant, however, we did not observe these differences in *FTO* obesity-risk carrier samples (Figures 3D–J). As compared to risk-free carriers, active beige adipocytes with *FTO* obesity-risk genotype had lower expression of these thermogenic genes and also that of the neurotrophic factor *S100b*, which was postulated to stimulate sympathetic axon growth and to play an important role in BAT innervation (Zeng et al., 2019) (Figures 3A–K). These results are in accordance with our RNA-seq data suggesting the critical importance of *FTO* rs1421085 SNP in active beige adipocytes and the compromised effect of active beige differentiation protocol in the presence of obesity-risk alleles.

3.4 Active beige adipocytes with *FTO* obesity-risk genotype expressed less amount of mitochondrial complex subunits and had lower proton leak respiration

Having observed that *FTO* rs1421085 SNP affected the expression of thermogenic genes, our next aim was to investigate whether the expression of mitochondrial complex subunits and cellular respiration were also suppressed in adipocytes with obesity-risk alleles. We found that active beige adipocytes carrying *FTO* risk-free genotype had higher amounts of mitochondrial complex subunits I, II, and IV as compared to white or inactive beige adipocytes carrying the same TT genotype (Figures 4A–C, E). However, no difference was found between the
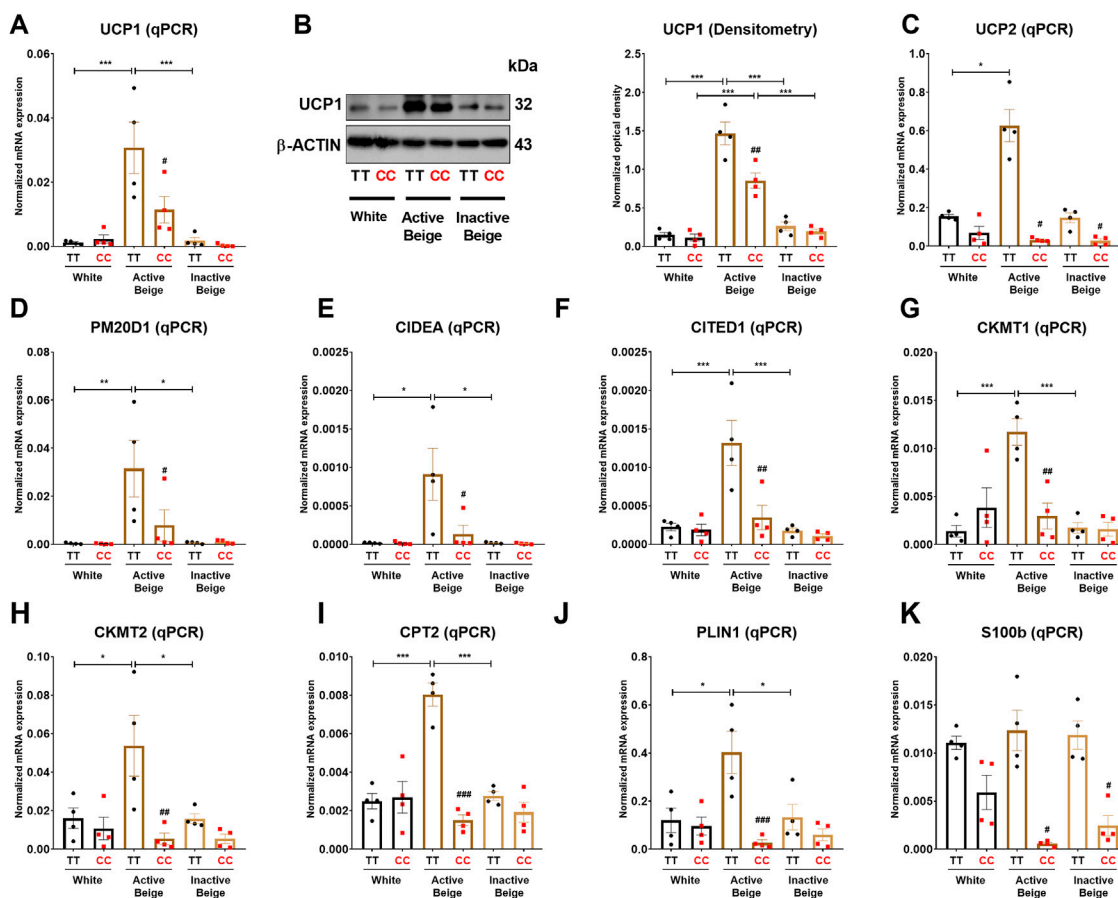
FIGURE 3
The effect of the differentiation protocols and alleles at *FTO* rs1421085 on the expression of thermogenesis markers in differentiated abdominal subcutaneous adipocytes. **(A, B)** The mRNA **(A)** and protein **(B)** expression of UCP1 measured by qPCR or immunoblotting. **(C–K)** The mRNA expression of *UCP2, PM20D1, CIDEA, CITED1, CKMT1* and *2, CPT2, PLIN1,* and *S100B* was analyzed by RT–qPCR. Statistical analysis was performed by ANOVA, n = 4 of each genotypes, */#$p < 0.05$, **/##$p < 0.01$, and ***/###$p < 0.001$. *analysis was performed to compare the effect of the applied differentiation protocol in the same genotype. #analysis was performed to compare *FTO* rs1421085 TT and CC genotypes within the same differentiation protocol.

three types of differentiation programs when adipocytes carried the obesity-risk variant (Figures 4A–C, E). Active beige adipocytes with *FTO* obesity-risk alleles had lower expression of mitochondrial complex subunits I, II, and IV as compared to the risk-free carriers (Figures 4A–C,E). We observed a similar but statistically not significant trend in the case of mitochondrial complex subunit III (Figure 4D), while the expression of complex V subunit was similar for all types of adipocytes regardless the *FTO* rs1421085 genotype (Figure 4F). Next, we measured the cellular respiration of the three types of adipocytes carrying *FTO* risk-free or obesity-risk alleles. In accordance with the mitochondrial complex subunit expression, we found that active beige adipocytes carrying risk-free genotype had higher respiration (at both basal and maximal stimulated conditions), stimulated proton leak respiration, and extracellular acidification as compared to white or inactive beige adipocytes, but this difference was not pronounced when the adipocytes carried the risk variant (Figures 4G, H). Stimulated ATP-dependent respiration was not affected significantly by either the applied differentiation protocols or the *FTO* rs1421085 genotype (Figure 4G). Active beige adipocytes with *FTO* obesity-risk variant showed lower cellular respiration,

especially stimulated proton leak respiration which reflects UCP1-dependent heat production, and extracellular acidification, which associates with glycolytic activity, as compared to risk-free carriers (Figures 4G, H). Intriguingly, the effect of *FTO* obesity-risk alleles on cellular respiration was observed in active beige but not in white or inactive beige adipocytes highlighting its exclusive effect in human abdominal SC adipocytes only when they are activated for thermogenesis.

3.5 Adipocytes carrying *FTO* obesity-risk genotype consume lower amounts of neutral amino acids when activated for thermogenesis

Active thermogenic adipocytes utilize metabolic substrates, such as carbohydrates, fatty acids, or amino acids to generate heat (Onogi and Ussar, 2022). Therefore, we aimed to investigate the fuel utilization by abdominal SC adipocytes with distinct *FTO* genotypes in three types of differentiation programs. Fatty acids are primarily released from lipid droplets via lipolysis (Cannon and
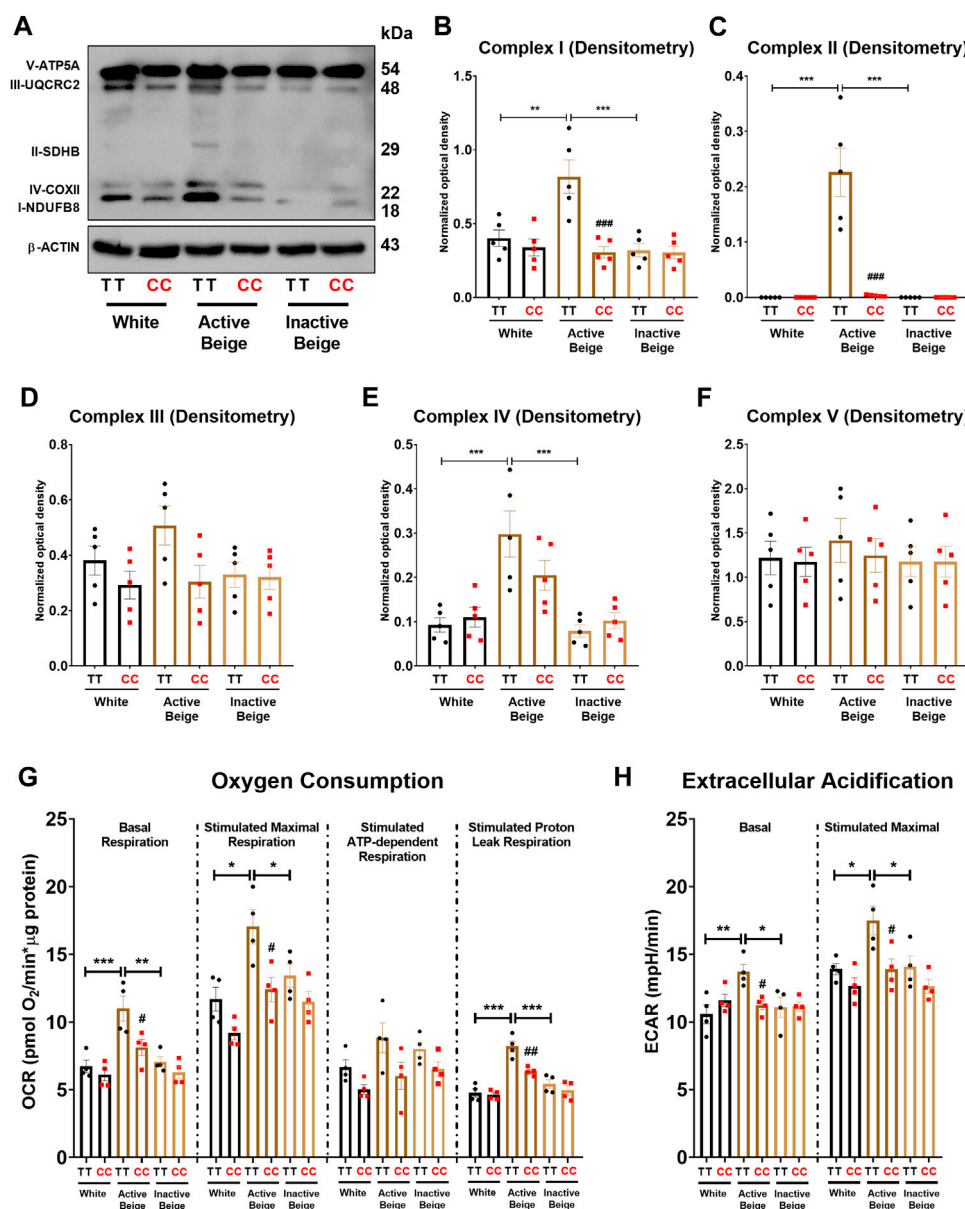
FIGURE 4
The effect of the differentiation protocols and alleles at *FTO* rs1421085 on the expression of mitochondrial complex subunits, oxygen consumption, and extracellular acidification. **(A–F)** Protein expression of mitochondrial complex subunits detected by immunoblotting. **(G, H)** Oxygen consumption at basal, dibutyryl-cAMP stimulated maximal, and stimulated proton leak respiration **(G)** and extracellular acidification **(H)** were quantified in white, active beige, and inactive beige adipocytes carrying *FTO* risk-free or obesity-risk genotypes by Seahorse extracellular flux analysis. Statistical analysis was performed by ANOVA, $n = 4$ of each genotypes, */#$p < 0.05$, **/##$p < 0.01$, and ***/###$p < 0.001$. *analysis was performed to compare the effect of the applied differentiation protocol in the same genotype. #analysis was performed to compare *FTO* rs1421085 TT and CC genotypes within the same differentiation protocol.

Nedergaard, 2004; Townsend and Tseng, 2014). We found that the regulation of lipolysis in adipocytes and fatty acid metabolism gene expression pathways were downregulated in active beige adipocytes with *FTO* CC as compared to TT allele carriers (Figure 2E). Although murine brown adipocytes can compensate the lack of lipid droplets-derived fatty acids (Chitraju et al., 2020), our *ex vivo* model did not include fatty acids in the applied differentiation media. Furthermore, stimulated etomoxir-sensitive oxygen consumption, which correlates with the activity of fatty acid oxidation (Nagy et al., 2022), was not affected significantly by

either the differentiation programs or the *FTO* genotypes (Supplementary Figure S4). ASC-1, which is encoded by *SLC7A10*, plays an important role in mediating alanine, serine, cysteine, and glycine consumption in human adipocytes derived from abdominal SC and deep neck regions (Jersin et al., 2021; Arianti et al., 2021). To evaluate the preferable energy sources during thermogenic activation, we monitored the oxygen consumption of adipocytes upon etomoxir (inhibitor of carnitine palmitoyltransferase-1) administration. ETO-R respiration, which reflects the activity of carbohydrate and amino acid oxidation (Nagy
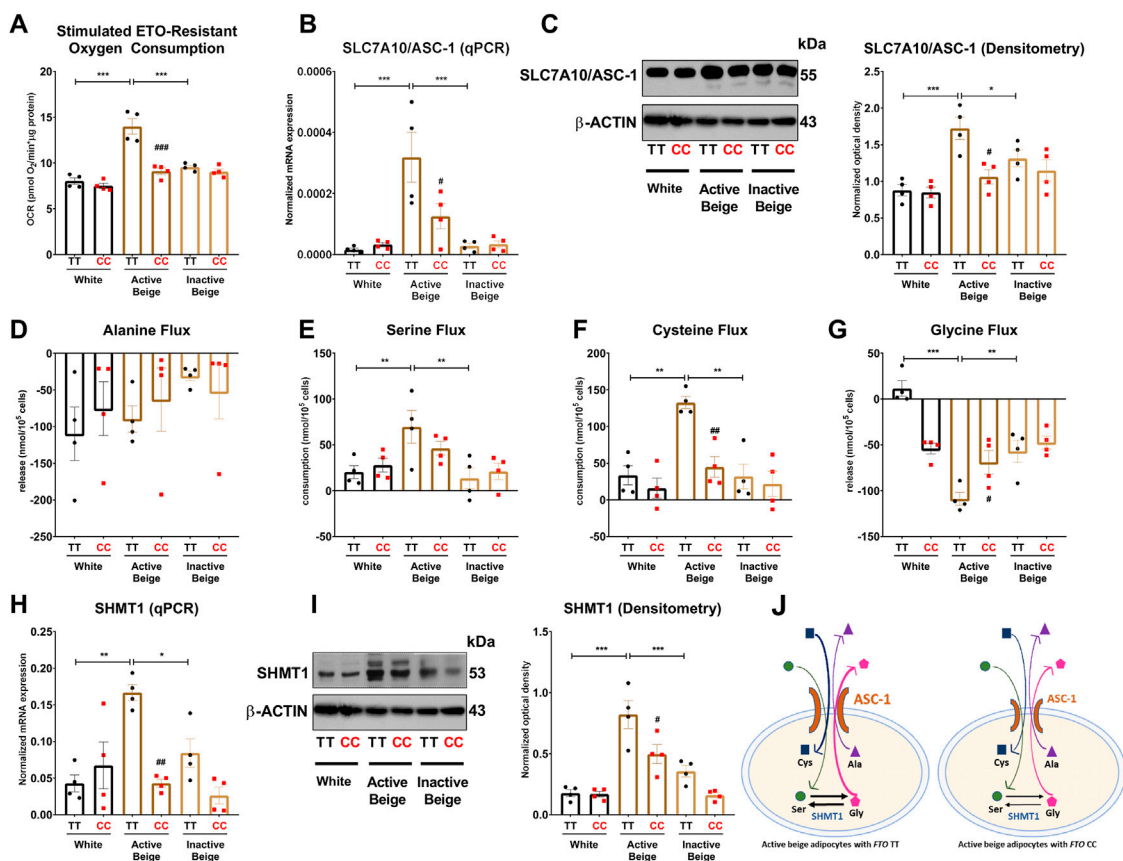
FIGURE 5
The effect of the differentiation protocols and alleles at *FTO* rs1421085 on the ASC-1-mediated amino acid flux and the expression of SHMT1 of differentiated abdominal subcutaneous adipocytes. **(A)** Etomoxir-resistant oxygen consumption was quantified in white, active beige, and inactive beige adipocytes carrying risk-free or obesity-risk genotypes by Seahorse extracellular flux analysis. **(B, C)** mRNA **(B)** and protein **(C)** expression of *SLC7A10/* ASC-1 by RT-qPCR and immunoblotting, $n = 4$ of each genotype. **(D–G)** Amino acids flux measured in the conditioned media of differentiated abdominal subcutaneous adipocytes, $n = 4$ of each genotype. **(H, I)** mRNA **(H)** and protein **(I)** expression of SHMT1 by RT-qPCR and immunoblotting, $n = 4$ of each genotype. **(J)** Graphical representation of ASC-1-mediated amino acid flux and SHMT1 enzyme activity in active beige adipocytes with *FTO* TT (left panel) and CC (right panel) alleles. Statistical analysis was performed by ANOVA. */#$p < 0.05$, **/##$p < 0.01$, and ***/###$p < 0.001$. *analysis was performed to compare the effect of the applied differentiation protocol in the same genotype. #analysis was performed to compare *FTO* rs1421085 TT and CC genotypes within the same differentiation protocol.

et al., 2022), was higher in active beige adipocytes with *FTO* risk-free genotype than in white or inactive beige adipocytes carrying the same TT genotype (Figure 5A). Active beige adipocytes with *FTO* obesity-risk alleles had lower level of ETO-R oxygen consumption as compared to risk-free carriers (Figure 5A). These observations suggest less pronounced carbohydrate and/or amino acid utilization in active beige adipocytes of CC carriers at *FTO* rs1421085.

Because we found *SLC7A10* (encoding alanine-serine-cysteine transporter, ASC-1) as a DEG among the most abundantly expressed genes in active beige adipocytes with *FTO* risk-free genotype (Figure 1H; Supplementary Table S7), we decided to investigate the effect of the applied differentiation protocols and *FTO* rs1421085 SNP on the expression of ASC-1 and the consumption of ASC-1 cargos by the adipocytes. We found that active beige adipocytes with risk-free alleles expressed higher mRNA level of *SLC7A10* as compared to white or inactive beige ones that carried the same TT variant (Figure 5B), which could be confirmed at ASC-1 protein level (Figure 5C). The presence of the *FTO*

rs1421085 SNP resulted in lower expression of *SLC7A10* in active beige adipocytes; this effect was statistically significant at protein level but not at mRNA level (Figures 5B,C). Next, we measured the consumption of amino acids in the conditioned media obtained from the three types of differentiated adipocytes with CC or TT alleles, respectively. The applied differentiation programs did not affect the release of alanine regardless of the *FTO* allele status (Figure 5D). In the case of adipocytes with *FTO* risk-free genotype, we found that active beige ones consumed higher amounts of serine (Figure 5E) and cysteine (Figure 5F) and released more glycine as compared to white or inactive beige adipocytes (Figure 5G). In accordance with the aforementioned gene expression and ETO-R oxygen consumption results, we did not observe any differences in the fluxes of these amino acids between the three types of differentiation protocols in adipocytes with obesity-risk alleles. Active beige adipocytes with obesity-risk genotype consumed lower amount of cysteine as compared to risk-free carriers (Figure 5F), but significant effect of the SNP was not observed on serine consumption (Figure 5E) suggesting
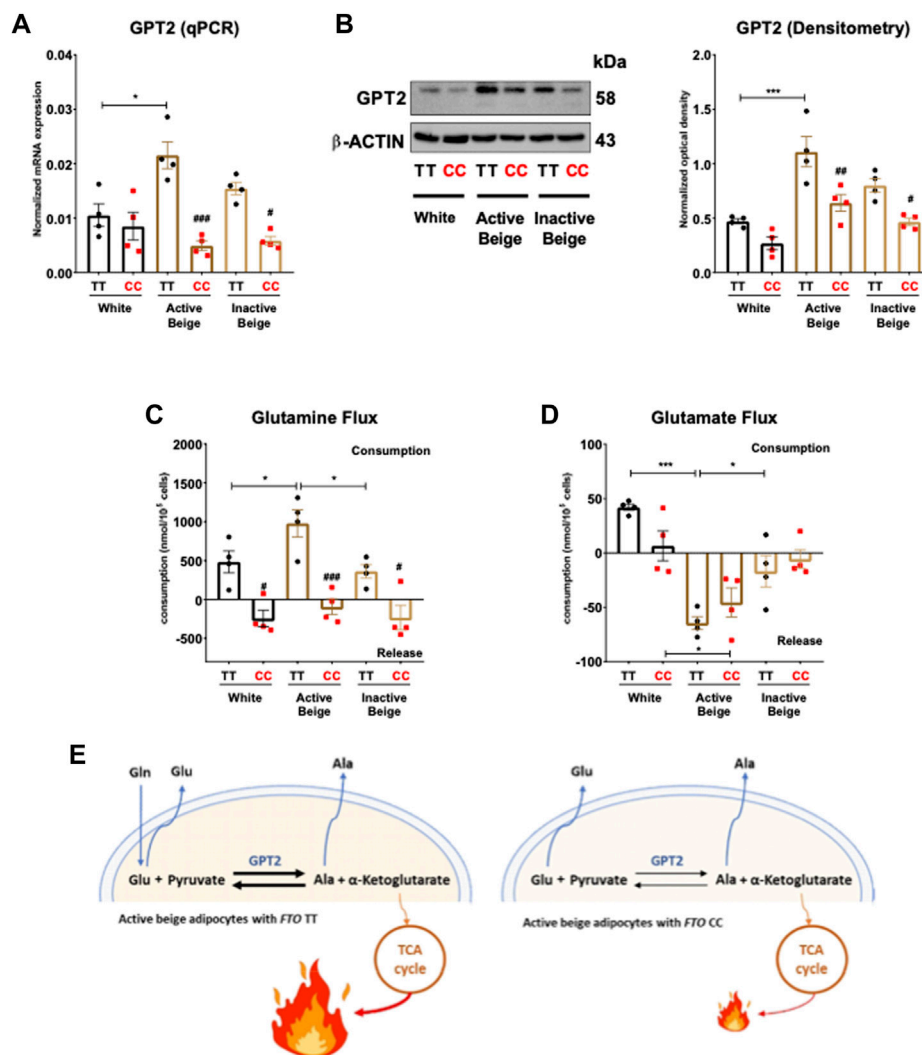
FIGURE 6
The effect of differentiation protocols and alleles at *FTO* rs1421085 on the expression of GPT2 and glutamine–glutamate flux of differentiated abdominal subcutaneous adipocytes. **(A, B)** mRNA **(A)** and protein **(B)** expression of GPT2 by RT-qPCR and immunoblotting, *n* = 4 of each genotype. **(C, D)** Glutamine **(C)** and glutamate **(D)** flux measured in the conditioned media of differentiated abdominal subcutaneous adipocytes, *n* = 4 of each genotypes. **(E)** Graphical representation of glutamine–glutamate flux and GPT2 enzyme activity in active beige adipocytes with *FTO* TT (left panel) and CC (right panel) alleles. Statistical analysis was performed by ANOVA. */#$p < 0.05$, **/##$p < 0.01$, and ***/###$p < 0.001$. *analysis was performed to compare the effect of the applied differentiation protocol in the same genotype. #analysis was performed to compare *FTO* rs1421085 TT and CC genotypes within the same differentiation protocol.

that other amino acid transporters might compensate for the reduced expression of ASC-1.

Our RNA-seq data showed that serine hydroxymethyltransferase (SHMT) 1, which catalyzes the conversions of L-serine and tetrahydrofolate (THF) to glycine and 5,10-methylene-THF (5,10-CH$_2$-THF), was expressed lower in active beige adipocytes with *FTO* obesity-risk as compared to risk-free carriers (Supplementary Table S5). We validated our RNA-seq data of SHMT1 expression by RT-qPCR (Figure 5H) and immunoblotting (Figure 5I). We also found that active beige adipocytes had higher protein content of SHMT1 as compared to white or inactive beige adipocytes in the presence of the *FTO* risk-free variant, but this difference was not observed in obesity-risk carrier samples (Figure 5I). The proposed model of ASC-1 mediated

amino acid flux and possible interconversion of serine and glycine by SHMT1 are summarized in Figure 5J.

According to the RNA-seq data, active beige adipocytes carrying obesity-risk genotype expressed lower mRNA level of glutamic pyruvic transaminase (GPT) 2 as compared to risk-free allele carriers (Supplementary Table S5). In the case of adipocytes with *FTO* risk-free alleles, active beige cells expressed more GPT2 both at mRNA (Figure 6A) and protein level (Figure 6B) as compared to white ones. We also observed lower expression of GPT2 in active and inactive beige adipocytes with *FTO* obesity-risk genotype as compared to risk-free allele carriers (Figures 6A, B). Active beige adipocytes carrying risk-free genotypes also consumed higher amount of glutamine as compared to white or inactive beige adipocytes carrying the same TT genotype, but no difference was

observed among the three types of differentiation protocols in the case of the samples with obesity-risk alleles. On the contrary to risk-free carrier cells, adipocytes with *FTO* obesity-risk genotype did not consume glutamine irrespective to the applied differentiation protocols (Figure 6C). In contrast, we found that active beige adipocytes released higher amount of glutamate as compared to inactive ones, while white adipocytes rather consumed that amino acid. The consumption of glutamate did not depend on the allelic discrimination at *FTO* rs1421085 locus (Figure 6D). In the case of adipocytes with TT alleles, active beige cells consumed less aspartate and more leucine than white or inactive beige ones, however, the consumption of asparagine, isoleucine, threonine, valine, histidine, lysine, tyrosine, tryptophan, proline, methionine, phenylalanine, and arginine was not significantly affected by the applied protocols. Histidine was consumed by adipocytes with risk-free alleles, however, it was released by obesity-risk allele carrier ones irrespective of the applied differentiation. The same trend was found in the case of lysine without observing statistically significant differences. Adipocytes with CC genotype tended to consume valine, however, it was released by the adipocytes with TT genotype. The *FTO* alleles did not affect the consumption of aspartate, asparagine, leucine, isoleucine, threonine, tyrosine, tryptophan, proline, methionine, phenylalanine, and arginine at a statistically significant level (Supplementary Figure S5). These results suggest that active beige adipocytes with *FTO* TT alleles utilize higher amounts of glutamine, which can be converted to glutamate, presumably to generate more of the TCA cycle intermediate, α-ketoglutarate which may contribute to elevated heat generation (Figure 6E).

4 Discussion

Abdominal fat is classified into SC and intraabdominal fat, which is mainly composed of visceral or intraperitoneal WAT (Mårin et al., 1992; Wajchenberg, 2000). Several studies reported that accumulation of visceral WAT is strongly associated with the risk of metabolic disorders (Matsuzawa et al., 1995; Fujimoto et al., 1994; Banerji et al., 1999), whereas other studies claimed that abdominal SC WAT may possess a protective role (McLaughlin et al., 2011; Patel and Abate, 2013). A more recent study using an elegant PET/CT technique, Leitner et al. (2017) reported that human BAT or brownable adipose tissue can be found in cervical, supraclavicular, axillary, mediastinal, paraspinal, and abdominal depots. In this study, we performed RNA-seq on human abdominal SC derived adipocytes with *FTO* rs1421085 risk-free or obesity-risk genotypes, which were differentiated by applying three types of protocols: white, active, or inactive beige. Irrespective to the *FTO* genotypes, we found that active beige adipocytes exerted greater thermogenic potential, marked by higher expression of thermogenic genes and browning capacity quantified by ProFAT, as compared to white or inactive beige cells. Our results suggest that human abdominal SC adipocytes have a significant thermogenic potential when they are activated using active beige differentiation protocol driven by a PPARγ agonist and adrenergic stimulation. However, this potential subsides when adipocytes are inactivated through beige to white transition. This is in line with our previous study which has reported that beige to white transition leads to

increased mitophagy resulting in the appearance of white-like phenotype and reduced thermogenesis (Vámos et al., 2022). Other studies also revealed that beige adipocytes in mice gradually lose their thermogenic morphology and capacity after the external stimuli, such as β-adrenergic agonist or cold exposure, were withdrawn (Altshuler-Keylin et al., 2016; Rosenwald et al., 2013). The loss of thermogenic characteristics in murine beige adipocytes was coupled with increased mitophagy, which was mediated by parkin (Lu et al., 2018; Sarraf and Youle, 2018). The comparison of active beige and white or inactive beige adipocytes found 100 and 164 genes, which were commonly more and less expressed, respectively, in active beige adipocytes. Notably, several well-known thermogenesis markers, such as *CITED1*, *PM20D1*, *PLIN5*, *GK*, and *AQP3* were commonly upregulated in active beige as compared to white or inactive beige adipocytes. No DEGs were found in the comparison of white and inactive beige adipocytes indicating a high similarity of the gene expression profiles in these two differentiation programs.

Dibutyryl-cAMP is extensively used to mimic *in vivo* thermogenesis due to its ability to penetrate the cell membrane (Cypess et al., 2013). In contrast to cAMP, which can be hydrolyzed by phosphodiesterase (PDE), dibutyryl-cAMP is resistant to degradation by PDE (Jarett and Smith, 1974; Blecher, 1971). cAMP activates protein kinase A (PKA), which phosphorylates various proteins and initiate consecutive cascades of additional protein kinases (Daniel et al., 1998). More recently, a role has emerged for PKA in the regulation of gene transcription (Daniel et al., 1998; London and Stratakis, 2022). When we administered dibutyryl-cAMP in the middle of active and inactive beige differentiation programs (at day 14 for 4 h) we found that the effect of the compound on the thermogenic gene expression was sustained until the end of the differentiation of active beige, but not in inactive beige (undergoing beige to white transition) adipocytes. This suggests that the effect of dibutyryl-cAMP can be maintained for a long period of time in beige adipocytes. Activation of cAMP response element binding protein (CREB) is one of the most studied links between PKA and gene expression regulation (Daniel et al., 1998). Daniel et al. (1998) described that cAMP increased the mRNA level of PDE, although the molecular mechanism of this regulation remained elusive. We also found that the expression of *PDE1B* was high in active beige adipocytes suggesting active cAMP-driven signaling. In another set of experiments, we found that the mRNA expression of *UCP1* was higher in active beige as compared to regularly differentiated beige adipocytes (28 days differentiation driven by rosiglitazone without dibutyryl-cAMP administration at day 14) (Supplementary Figure S6) suggesting that dibutytyl-cAMP treatment at the middle of beige differentiation program further enhances the thermogenic capacity of abdominal SC adipocytes at a sustained manner.

We also evaluated the effect of rs1421085 T-to-C SNP of the *FTO* gene, which interrupts a conserved motif for ARID5B repressor, resulting in elevated expression of IRX3 and IRX5 during the early stage of adipocyte differentiation. As the consequence, the commitment of the cells diverts from beige towards the white program and lipid storage increases (Claussnitzer et al., 2015). When the gene expression profiles of the three types of adipocytes were analyzed by segregating the *FTO* rs1421085 risk-free (TT) and obesity-risk (CC) allele carrier

samples, intriguingly, we found that the SNP affected the gene expression profile, in particular the expression of thermogenic markers (*CITED1*, *CIDEC*, *PLIN1*, *LIPE, CKMT2*, and *S100b*), in active beige adipocytes, but not in white or inactive beige adipocytes. CIDEC, PLIN1, and LIPE are lipid droplet-associated proteins, which regulate triglyceride accumulation and lipolysis (Wolins et al., 2006; Puri et al., 2008). Decreased expression of these genes in active beige adipocytes with *FTO* obesity-risk alleles may contribute to the downregulation of lipolysis in the SC adipose tissue of affected individuals. CKMT1a/b and CKMT2 mitochondrial creatine kinases phosphorylate creatine generating phosphocreatine and contribute to UCP1-independent heat generation via creatine futile cycle (Kazak et al., 2015). S100b protein was proposed to play a role in the sympathetic innervation of thermogenic adipose tissue by stimulating neurite outgrowth from sympathetic neurons through calsyntenin (CLSTN) 3β axis (Zeng et al., 2019). Reduced expression or loss of function of S100b resulted in disrupted sympathetic innervation leading to reduced thermogenesis in brown or beige adipocytes. Of note, recently, it was shown that adipose tissue specific CLSTN3β$^{-/-}$ mice did not have defects in the sympathetic innervation and adrenergic signaling of BAT (Qian et al., 2023). Decreased expression of S100b in abdominal SC adipocytes with *FTO* obesity-risk carriers, however, might partially contribute to lower thermogenic capacity in abdominal SC WAT even when the adipocytes are activated for heat production. Importantly, genes overrepresented in metabolic, especially in energy metabolism-related pathways, such as TCA cycle, lipolysis, pyruvate metabolism, and PPAR signaling were downregulated in active beige adipocytes with obesity-risk genotypes as compared to risk-free allele carriers, indicating lower energy dissipation in active beige adipocytes with CC alleles. Our findings suggest that C alleles at *FTO* rs1421085 suppress the thermogenic activation of human abdominal SC adipocytes; even long-term rosiglitazone treatment could not compensate for the effect of the obesity-risk genotype. In addition, we also observed that active beige adipocytes carrying *FTO* obesity-risk alleles exerted similar transcriptomic profiles as white or inactive beige adipocytes. This is in association with our previous study, which reported that the thermogenically prone human neck derived adipocytes carrying *FTO* obesity-risk genotype had lower expression of thermogenic genes, such as *CKMT1A/B*, *CITED1*, *PPARGC1A/B*, and *CPT1B* and genes involved in respiratory electron transport, fatty acid metabolism, and the signaling by retinoic acid pathways (Tóth et al., 2020).

Active heat producing adipocytes utilize higher amounts of nutrients, such as glucose, fatty acids, and amino acids to provide sufficient fuel for thermogenesis and solute carrier (SLC) transporters play a crucial role in mediating the transport of these molecules (Cypess et al., 2009; Virtanen et al., 2009; Wu et al., 2006; Yoneshiro et al., 2019). Our data showed that active beige adipocytes carrying risk-free genotype had higher ETO-R oxygen consumption that reflects carbohydrate and amino acid utilization and expressed higher level of the neutral amino acid transporter, ASC-1 (encoded by *SLC7A10*) as compared to white or inactive beige adipocytes with the same TT genotypes, whereas there was no difference when the three types of adipocytes with *FTO* obesity-risk alleles were compared. ASC-1 has been recently identified as a novel regulator of energy metabolism in human SC adipose tissue

elevating mitochondrial respiration and preventing development of adipocyte hypertrophy and insulin resistance (Jersin et al., 2021). Our previous study reported that ASC-1-mediated uptake of serine, cysteine, and glycine is essential for efficient thermogenic response upon adrenergic stimulation in human neck derived adipocytes (Arianti et al., 2021). The role of ASC-1 in adipose tissue has been comprehensively reviewed by Jersin et al. (2022) highlighting its beneficial effects in enhancing mitochondrial activity and lowering reactive oxygen species production in white adipocytes. We also found that the consumption of serine and cysteine was higher in active beige as compared to white or inactive beige adipocytes with *FTO* risk-free genotype. Lower consumption of these amino acids was observed in active beige adipocytes with *FTO* obesity-risk genotype as compared to risk-free allele carriers. In addition, we observed release of less glycine by active beige adipocytes carrying obesity-risk genotypes as compared to those with risk-free alleles. Serine is an important metabolic source to generate one-carbon units in mammalian cells (de Koning et al., 2003), which are produced by both isoforms of SHMT enzymes, SHMT1 (cytosolic) and SHMT2 (mitochondrial), resulting in glycine. Our data showed that active beige adipocytes carrying *FTO* obesity-risk genotype expressed lower level of SHMT1 as compared to risk-free allele carrier ones suggesting lower generation of one-carbon units in thermogenic adipocytes with *FTO* obesity-risk genotype. We also revealed that one-carbon metabolism pathway, in which SHMT1 and GPT2 participate, was less expressed in active beige adipocytes with *FTO* obesity-risk alleles. One-carbon unit metabolism forms a functional interaction with mitochondrial oxidative phosphorylation that is crucial for ATP or heat generation in mammalian cells (Lucas et al., 2018). Lower serine influx that can result in the decrease of one-carbon unit levels may lead to lower amounts of mitochondrial complex subunits I, II, and IV in active beige adipocytes carrying *FTO* obesity-risk genotype. As a consequence, stimulated maximal and proton leak respiration, which positively correlates with UCP1 activity, and extracellular acidification were suppressed in active beige adipocytes originated from *FTO* obesity-risk genotype carriers.

Active beige adipocytes with risk-free genotype also consumed higher amounts of glutamine as compared to white or inactive beige adipocytes carrying the same alleles. The *FTO* obesity-risk carrier adipocytes did not consume glutamine irrespective of the differentiation protocol used. Glutamine is the most abundant free amino acid in the circulation (Hall et al., 1996) and in the applied DMEM-F12 cell culture medium. It is one of the main fuel resources for cells supplying carbon atoms to drive the TCA cycle and generate ATP (or heat) (Scalise et al., 2016). Lower expression of *GPT2* and glutamine consumption may contribute to the downregulation of pyruvate metabolism and TCA cycle pathway in active beige adipocytes with obesity-risk alleles. In addition, sodium-dependent neutral amino acid transporter type 2 (ASCT2)/SLC1A5-mediated glutamine uptake is important for histone acetylation and methylation in murine WAT. Downregulation of ASCT2 as the consequence of disrupted PPAR-γ expression in WAT of obese mice led to reduced glutamine uptake and correlated with decreased H3K27ac and H3K4me3 at the *Bmal1* promoter (Wang et al., 2022). A recent publication reported that disrupted function of adipocyte ASC-1 led to the elevation of lipid storage and diverted adipocytes from releasing to consuming glutamate and aspartate (Jersin et al., 2023). Our data showed that active beige

adipocytes with risk-free *FTO* genotype, which expressed the highest level of ASC-1, consumed less aspartate as compared to white or inactive beige adipocytes. In contrast to white adipocytes that consumed glutamate, active beige adipocytes released it into the extracellular space. Altogether, our findings suggest that adipocytes derived from abdominal SC tissues of *FTO* obesity-risk carriers exert lower uptake of several amino acids as substrates of cellular metabolic processes contributing to compromised energy dissipation.

The positive correlation between *FTO* rs1421085 SNP and obesity or increased body mass index has been reported in several populations such as Estonian children (Katus et al., 2020), Chinese children (Wang et al., 2013), Iranian adults (Najd-Hassan-Bonab et al., 2022), Arabic (Hebbar et al., 2020), Pakistani (Rana and Bhatti, 2020), Balinese (Priliani et al., 2020), and Mexican Mayan girls (González-Herrera et al., 2019). Through genome-wide association meta-analyses of more than 100000 individuals of European ancestry without diabetes, *FTO* rs1421085 SNP was found to be significantly associated with fasting insulin levels (Scott et al., 2012). A recently published study by Laber et al. (2021) showed that an engineered deletion of the rs1421085 conserved cis-regulatory module in mice prevented high fat diet-induced obesity, decreased whole-body fat mass, and elevated the number of mitochondria in WAT. Our presented data highlight the critical effect of *FTO* rs1421085 SNP on human abdominal SC adipocytes only when they are activated for thermogenesis. Leitner *et al.* (2017) reported that large amounts of brownable adipocytes can be found in abdominal SC fat whose *in vivo* relevance in humans is still unrevealed. Furthermore, the activation of these adipocytes in humans to reduce adiposity remains challenging. Although these cells can be potentially activated, our previous (Tóth et al., 2020) and present results have pointed to a strong effect of obesity-risk genotype at *FTO* rs1421085 SNP, which has a high prevalence in the European population (Dina et al., 2007; Babenko et al., 2019; Hudek et al., 2017) and Mexican children (12.93%–18.67%) (González-Herrera et al., 2019) that must be overcome to enable efficient thermogenesis and weight loss. Our findings further support the importance of genetic background not only in the pathogenesis of obesity but also in the potential effectivity of novel therapeutic approaches which target thermogenesis-related energy dissipation.

Data availability statement

The RNA-seq datasets generated and analyzed for this study can be found in the Sequence Read Archive (SRA) database [https://www.ncbi.nlm.nih.gov/sra] under accession number PRJNA928240.

Ethics statement

The studies involving human participants were reviewed and approved by Medical Research Council of Hungary (20571-2/2017/

EKU). The patients/participants provided their written informed consent to participate in this study.

Author contributions

AV, RiA, BV, RaA, AS performed the experiments. EK, RiA, and AV conceptualized the research, with inputs from LF. SP performed the RNA-seq. AG and ÉC carried out measurements of amino acid concentration. IC and GM acquired and analyzed confocal microscopy images. CL and ZB provided adipose tissue samples. EK and LF supervised the research and acquired funding. RiA and AV wrote the original draft of the manuscript. EK and LF edited the final version of the manuscript. All authors contributed to the article and approved the submitted version.

Conflict of interest

The authors declare that the research was conducted in the absence of any commercial or financial relationships that could be construed as a potential conflict of interest.

Publisher's note

All claims expressed in this article are solely those of the authors and do not necessarily represent those of their affiliated organizations, or those of the publisher, the editors and the reviewers. Any product that may be evaluated in this article, or claim that may be made by its manufacturer, is not guaranteed or endorsed by the publisher.

Supplementary material

The Supplementary Material for this article can be found online at: https://www.frontiersin.org/articles/10.3389/fcell.2023.1155673/full#supplementary-material

References

Altshuler-Keylin, S., Shinoda, K., Hasegawa, Y., Ikeda, K., Hong, H., Kang, Q., et al. (2016). Beige adipocyte maintenance is regulated by autophagy-induced mitochondrial clearance. *Cell Metab.* 24 (3), 402–419. doi:10.1016/j.cmet.2016.08.002

Arianti, R., Vinnai, B. Á., Tóth, B. B., Shaw, A., Csősz, É., Vámos, A., et al. (2021). ASC-1 transporter-dependent amino acid uptake is required for the efficient thermogenic response of human adipocytes to adrenergic stimulation. *FEBS Lett.* 595 (16), 2085–2098. doi:10.1002/1873-3468.14155

Babenko, V., Babenko, R., Gamieldien, J., and Markel, A. (2019). FTO haplotyping underlines high obesity risk for European populations. *BMC Med. Genomics* 12 (Suppl. 2), 46. doi:10.1186/s12920-019-0491-x

Banerji, M. A., Faridi, N., Atluri, R., Chaiken, R. L., and Lebovitz, H. E. (1999). Body composition, visceral fat, leptin, and insulin resistance in Asian Indian men. *J. Clin. Endocrinol. Metab.* 84 (1), 137–144. doi:10.1210/jcem.84.1.5371

Bjune, J. I., Dyer, L., Røsland, G. V., Tronstad, K. J., Njølstad, P. R., Sagen, J. V., et al. (2020). The homeobox factor Irx3 maintains adipogenic identity. *Metab. Clin. Exp.* 103, 154014. doi:10.1016/j.metabol.2019.154014

Blecher, M. (1971). Biological effects and catabolic metabolism of 3′,5′-cyclic nucleotides and derivatives in rat adipose tissue and liver. *Metab. Clin. Exp.* 20 (1), 63–77. doi:10.1016/0026-0495(71)90060-6

Cannon, B., and Nedergaard, J. (2004). Brown adipose tissue: Function and physiological significance. *Physiol. Rev.* 84 (1), 277–359. doi:10.1152/physrev.00015.2003

Chan, M., Lim, Y. C., Yang, J., Namwanje, M., Liu, L., and Qiang, L. (2019). Identification of a natural beige adipose depot in mice. *J. Biol. Chem.* 294 (17), 6751–6761. doi:10.1074/jbc.RA118.006838

Cheng, L., Wang, J., Dai, H., Duan, Y., An, Y., Shi, L., et al. (2021). Brown and beige adipose tissue: A novel therapeutic strategy for obesity and type 2 diabetes mellitus. *Adipocyte* 10 (1), 48–65. doi:10.1080/21623945.2020.1870060

Cheng, Y., Jiang, L., Keipert, S., Zhang, S., Hauser, A., Graf, E., et al. (2018). Prediction of adipose browning capacity by systematic integration of transcriptional profiles. *Cell Rep.* 23 (10), 3112–3125. doi:10.1016/j.celrep.2018.05.021

Chitraju, C., Fischer, A. W., Farese, R. V., Jr, and Walther, T. C. (2020). Lipid droplets in Brown adipose tissue are dispensable for cold-induced thermogenesis. *Cell Rep.* 33 (5), 108348. doi:10.1016/j.celrep.2020.108348

Christakis, N. A., and Fowler, J. H. (2007). The spread of obesity in a large social network over 32 years. *N. Engl. J. Med.* 357 (4), 370–379. doi:10.1056/NEJMsa066082

Claussnitzer, M., Dankel, S. N., Kim, K. H., Quon, G., Meuleman, W., Haugen, C., et al. (2015). FTO obesity variant circuitry and adipocyte browning in humans. *N. Engl. J. Med.* 373 (10), 895–907. doi:10.1056/NEJMoa1502214

Cypess, A. M., Lehman, S., Williams, G., Tal, I., Rodman, D., Goldfine, A. B., et al. (2009). Identification and importance of Brown adipose tissue in adult humans. *N. Engl. J. Med.* 360 (15), 1509–1517. doi:10.1056/NEJMoa0810780

Cypess, A. M., White, A. P., Vernochet, C., Schulz, T. J., Xue, R., Sass, C. A., et al. (2013). Anatomical localization, gene expression profiling and functional characterization of adult human neck Brown fat. *Nat. Med.* 19 (5), 635–639. doi:10.1038/nm.3112

Daniel, P. B., Walker, W. H., and Habener, J. F. (1998). Cyclic AMP signaling and gene regulation. *Annu. Rev. Nutr.* 18, 353–383. doi:10.1146/annurev.nutr.18.1.353

de Koning, T. J., Snell, K., Duran, M., Berger, R., Poll-The, B. T., and Surtees, R. (2003). L-serine in disease and development. *Biochem. J.* 371 (Pt 3), 653–661. doi:10.1042/BJ20021785

Dina, C., Meyre, D., Gallina, S., Durand, E., Körner, A., Jacobson, P., et al. (2007). Variation in FTO contributes to childhood obesity and severe adult obesity. *Nat. Genet.* 39 (6), 724–726. doi:10.1038/ng2048

Felix, J. F., Bradfield, J. P., Monnereau, C., van der Valk, R. J., Stergiakouli, E., Chesi, A., et al. Bone Mineral Density in Childhood Study BMDCS (2016). Genome-wide association analysis identifies three new susceptibility loci for childhood body mass index. *Hum. Mol. Genet.* 25(2), 389–403. doi:10.1093/hmg/ddv472

Frayling, T. M., Timpson, N. J., Weedon, M. N., Zeggini, E., Freathy, R. M., Lindgren, C. M., et al. (2007). A common variant in the FTO gene is associated with body mass index and predisposes to childhood and adult obesity. *Sci. (New York, N.Y.)* 316 (5826), 889–894. doi:10.1126/science.1141634

Frühbeck, G., Kiortsis, D. N., and Catalán, V. (2018). Precision medicine: Diagnosis and management of obesity. *Diabetes and Endocrinol.* 6 (3), 164–166. doi:10.1016/S2213-8587(17)30312-1

Frühbeck, G., Toplak, H., Woodward, E., Yumuk, V., Maislos, M., Oppert, J. M., et al. (2013). Obesity: The gateway to ill health - an EASO position statement on a rising public health, clinical and scientific challenge in europe. *Obes. facts*, 6(2), 117–120. doi:10.1159/000350627

Fujimoto, W. Y., Abbate, S. L., Kahn, S. E., Hokanson, J. E., and Brunzell, J. D. (1994). The visceral adiposity syndrome in Japanese-American men. *Obes. Res.* 2 (4), 364–371. doi:10.1002/j.1550-8528.1994.tb00076.x

González-Herrera, L., Zavala-Castro, J., Ayala-Cáceres, C., Pérez-Mendoza, G., López-González, M. J., Pinto-Escalante, D., et al. (2019). Genetic variation of FTO: rs1421085 T>C, rs8057044 G>A, rs9939609 T>A, and copy number (CNV) in Mexican mayan school-aged children with obesity/overweight and with normal weight. *Am. J. Hum. Biol. Off. J. Hum. Biol. Counc.* 31 (1), e23192. doi:10.1002/ajhb.23192

Guba, A., Bába, O., Tőzsér, J., Csősz, É., and Kalló, G. (2022). Fast and sensitive quantification of AccQ-tag derivatized amino acids and biogenic amines by UHPLC-UV analysis from complex biological samples. *Metabolites* 12 (3), 272. doi:10.3390/metabo12030272

Hall, J. C., Heel, K., and McCauley, R. (1996). Glutamine. *Br. J. Surg.* 83 (3), 305–312. doi:10.1002/bjs.1800830306

Heaton, J. M. (1972). The distribution of Brown adipose tissue in the human. *J. Anat.* 112 (Pt 1), 35–39.

Hebbar, P., Abu-Farha, M., Mohammad, A., Alkayal, F., Melhem, M., Abubaker, J., et al. (2020). FTO variant rs1421085 associates with increased body weight, soft lean mass, and total body water through interaction with ghrelin and apolipoproteins in arab population. *Front. Genet.* 10, 1411. doi:10.3389/fgene.2019.01411

Herman, M. A., and Rosen, E. D. (2015). Making biological sense of GWAS data: Lessons from the FTO locus. *Cell metab.* 22 (4), 538–539. doi:10.1016/j.cmet.2015.09.018

Heymsfield, S. B., and Wadden, T. A. (2017). Mechanisms, pathophysiology, and management of obesity. *N. Engl. J. Med.* 376 (3), 254–266. doi:10.1056/NEJMra1514009

Huđek, A., Škara, L., Smolkovič, B., Kazazić, S., Ravlić, S., Nanić, L., et al. (2017). Higher prevalence of FTO gene risk genotypes AA rs9939609, CC rs1421085, and GG rs17817449 and saliva containing *Staphylococcus aureus* in obese women in Croatia. *Nutr. Res. (New York, N.Y.)* 50, 94–103. doi:10.1016/j.nutres.2017.12.005

Imamura, M., Takahashi, A., Yamauchi, T., Hara, K., Yasuda, K., Grarup, N., et al. (2016). Genome-wide association studies in the Japanese population identify seven novel loci for type 2 diabetes. *Nat. Commun.* 7, 10531. doi:10.1038/ncomms10531

Jarett, L., and Smith, R. M. (1974). Mode of action of N6-O2′-dibutyryl cyclic 3′,5′ AMP on fat cell metabolism. *Diabetes* 23 (1), 29–40. doi:10.2337/diab.23.1.29

Jersin, R. Å., Jonassen, L. R., and Dankel, S. N. (2022). The neutral amino acid transporter SLC7A10 in adipose tissue, obesity and insulin resistance. *Front. Cell Dev. Biol.* 10, 974338. doi:10.3389/fcell.2022.974338

Jersin, R. Å., Tallapragada, D. S. P., Madsen, A., Skartveit, L., Fjære, E., McCann, A., et al. (2021). Role of the neutral amino acid transporter SLC7A10 in adipocyte lipid storage, obesity, and insulin resistance. *Diabetes* 70 (3), 680–695. doi:10.2337/db20-0096

Jersin, R. Å., Tallapragada, D. S. P., Skartveit, L., Bjune, M. S., Muniandy, M., Lee-Ødegård, S., et al. (2023). Impaired transporter SLC7A10 promotes lipid storage in association with insulin resistance and altered BCAA metabolism. *J. Clin. Endocrinol. metabolism*, dgad148. Advance online publication. doi:10.1210/clinem/dgad148

Katus, U., Villa, I., Ringmets, I., Vaht, M., Mäestu, E., Mäestu, J., et al. (2020). Association of FTO rs1421085 with obesity, diet, physical activity, and socioeconomic status: A longitudinal birth cohort study. *Nutr. Metab. Cardiovasc. Dis.* 30 (6), 948–959. doi:10.1016/j.numecd.2020.02.008

Kazak, L., Chouchani, E. T., Jedrychowski, M. P., Erickson, B. K., Shinoda, K., Cohen, P., et al. (2015). A creatine-driven substrate cycle enhances energy expenditure and thermogenesis in beige fat. *Cell* 163 (3), 643–655. doi:10.1016/j.cell.2015.09.035

Klusóczki, Á., Veréb, Z., Vámos, A., Fischer-Posovszky, P., Wabitsch, M., Bacso, Z., et al. (2019). Differentiating SGBS adipocytes respond to PPARγ stimulation, irisin and BMP7 by functional browning and beige characteristics. *Sci. Rep.* 9 (1), 5823. doi:10.1038/s41598-019-42256-0

Kristóf, E., Doan-Xuan, Q. M., Bai, P., Bacso, Z., and Fésüs, L. (2015). Laser-scanning cytometry can quantify human adipocyte browning and proves effectiveness of irisin. *Sci. Rep.* 5, 12540. doi:10.1038/srep12540

Kristóf, E., Klusóczki, Á., Veress, R., Shaw, A., Combi, Z. S., Varga, K., et al. (2019). Interleukin-6 released from differentiating human beige adipocytes improves browning. *Exp. Cell Res.* 377 (1-2), 47–55. doi:10.1016/j.yexcr.2019.02.015

Laber, S., Forcisi, S., Bentley, L., Petzold, J., Moritz, F., Smirnov, K. S., et al. (2021). Linking the FTO obesity rs1421085 variant circuitry to cellular, metabolic, and organismal phenotypes *in vivo*. *Sci. Adv.* 7 (30), eabg0108. doi:10.1126/sciadv.abg0108

Leitner, B. P., Huang, S., Brychta, R. J., Duckworth, C. J., Baskin, A. S., McGehee, S., et al. (2017). Mapping of human Brown adipose tissue in lean and obese young men. *Proc. Natl. Acad. Sci. U. S. A.* 114 (32), 8649–8654. doi:10.1073/pnas.1705287114

Lin, X., and Li, H. (2021). Obesity: Epidemiology, pathophysiology, and therapeutics. *Front. Endocrinol.* 12, 706978. doi:10.3389/fendo.2021.706978

London, E., and Stratakis, C. A. (2022). The regulation of PKA signaling in obesity and in the maintenance of metabolic health. *Pharmacol. Ther.* 237, 108113. doi:10.1016/j.pharmthera.2022.108113

Lu, X., Altshuler-Keylin, S., Wang, Q., Chen, Y., Henrique Sponton, C., Ikeda, K., et al. (2018). Mitophagy controls beige adipocyte maintenance through a Parkin-dependent

and UCP1-independent mechanism. *Sci. Signal.* 11 (527), eaap8526. doi:10.1126/scisignal.aap8526

Lucas, S., Chen, G., Aras, S., and Wang, J. (2018). Serine catabolism is essential to maintain mitochondrial respiration in mammalian cells. *Life Sci. Alliance* 1 (2), e201800036. doi:10.26508/lsa.201800036

Mårin, P., Andersson, B., Ottosson, M., Olbe, L., Chowdhury, B., Kvist, H., et al. (1992). The morphology and metabolism of intraabdominal adipose tissue in men. *Metab. Clin. Exp.* 41 (11), 1242–1248. doi:10.1016/0026-0495(92)90016-4

Matsuzawa, Y., Shimomura, I., Nakamura, T., Keno, Y., Kotani, K., and Tokunaga, K. (1995). Pathophysiology and pathogenesis of visceral fat obesity. *Obes. Res.* 3 (Suppl. 2), 187S–194S. doi:10.1002/j.1550-8528.1995.tb00462.x

McLaughlin, T., Lamendola, C., Liu, A., and Abbasi, F. (2011). Preferential fat deposition in subcutaneous versus visceral depots is associated with insulin sensitivity. *J. Clin. Endocrinol. Metab.* 96 (11), E1756–E1760. doi:10.1210/jc.2011-0615

Mills, E. L., Pierce, K. A., Jedrychowski, M. P., Garrity, R., Winther, S., Vidoni, S., et al. (2018). Accumulation of succinate controls activation of adipose tissue thermogenesis. *Nature* 560 (7716), 102–106. doi:10.1038/s41586-018-0353-2

Nagy, L., Rauch, B., Szerafin, T., Uray, K., Tóth, A., and Bai, P. (2022). Nicotinamide-riboside shifts the differentiation of human primary white adipocytes to beige adipocytes impacting substrate preference and uncoupling respiration through SIRT1 activation and mitochondria-derived reactive species production. *Front. Cell Dev. Biol.* 10, 979330. doi:10.3389/fcell.2022.979330

Najd-Hassan-Bonab, L., Safarpour, M., Moazzam-Jazi, M., Azizi, F., and Daneshpour, M. S. (2022). The role of FTO variant rs1421085 in the relationship with obesity: A systematic review and meta-analysis. *Eat. Weight Disord.* 27, 3053–3062. Advance online publication. doi:10.1007/s40519-022-01509-0

Nokhoijav, E., Guba, A., Kumar, A., Kunkli, B., Kalló, G., Káplár, M., et al. (2022). Metabolomic analysis of serum and tear samples from patients with obesity and type 2 diabetes mellitus. *Int. J. Mol. Sci.* 23 (9), 4534. doi:10.3390/ijms23094534

Onogi, Y., and Ussar, S. (2022). Regulatory networks determining substrate utilization in Brown adipocytes. *Trends Endocrinol. Metab.* 33 (7), 493–506. doi:10.1016/j.tem.2022.04.001

Panic, V., Pearson, S., Banks, J., Tippetts, T. S., Velasco-Silva, J. N., Lee, S., et al. (2020). Mitochondrial pyruvate carrier is required for optimal Brown fat thermogenesis. *eLife* 9, e52558. doi:10.7554/eLife.52558

Patel, P., and Abate, N. (2013). Body fat distribution and insulin resistance. *Nutrients* 5 (6), 2019–2027. doi:10.3390/nu5062019

Perdikari, A., Leparc, G. G., Balaz, M., Pires, N. D., Lidell, M. E., Sun, W., et al. (2018). BATLAS: Deconvoluting Brown adipose tissue. *Cell Rep.* 25 (3), 784–797. doi:10.1016/j.celrep.2018.09.044

Petrovic, N., Walden, T. B., Shabalina, I. G., Timmons, J. A., Cannon, B., and Nedergaard, J. (2010). Chronic peroxisome proliferator-activated receptor gamma (PPARgamma) activation of epididymally derived white adipocyte cultures reveals a population of thermogenically competent, UCP1-containing adipocytes molecularly distinct from classic Brown adipocytes. *J. Biol. Chem.* 285 (10), 7153–7164. doi:10.1074/jbc.M109.053942

Pisani, D. F., Barquissau, V., Chambard, J. C., Beuzelin, D., Ghandour, R. A., Giroud, M., et al. (2018). Mitochondrial fission is associated with UCP1 activity in human brite/beige adipocytes. *Mol. Metab.* 7, 35–44. doi:10.1016/j.molmet.2017.11.007

Priliani, L., Oktavianthi, S., Hasnita, R., Nussa, H. T., Inggriani, R. C., Febinia, C. A., et al. (2020). Obesity in the Balinese is associated with FTO rs9939609 and rs1421085 single nucleotide polymorphisms. *PeerJ* 8, e8327. doi:10.7717/peerj.8327

Puri, V., Ranjit, S., Konda, S., Nicoloro, S. M., Straubhaar, J., Chawla, A., et al. (2008). Cidea is associated with lipid droplets and insulin sensitivity in humans. *Proc. Natl. Acad. Sci. U. S. A.* 105 (22), 7833–7838. doi:10.1073/pnas.0802063105

Qian, K., Tol, M. J., Wu, J., Uchiyama, L. F., Xiao, X., Cui, L., et al. (2023). CLSTN3β enforces adipocyte multilocularity to facilitate lipid utilization. *Nature* 613 (7942), 160–168. doi:10.1038/s41586-022-05507-1

Rana, S., and Bhatti, A. A. (2020). Association and interaction of the FTO rs1421085 with overweight/obesity in a sample of Pakistani individuals. *Eat Weight Disord.* 25 (5), 1321–1332. doi:10.1007/s40519-019-00765-x

Rosenwald, M., Perdikari, A., Rülicke, T., and Wolfrum, C. (2013). Bi-directional interconversion of brite and white adipocytes. *Nat. Cell Biol.* 15 (6), 659–667. doi:10.1038/ncb2740

Sanchez-Gurmaches, J., Hung, C. M., and Guertin, D. A. (2016). Emerging complexities in adipocyte origins and identity. *Trends Cell Biol.* 26 (5), 313–326. doi:10.1016/j.tcb.2016.01.004

Sarraf, S. A., and Youle, R. J. (2018). Parkin mediates mitophagy during beige-to-white fat conversion. *Sci. Signal.* 11 (527), eaat1082. doi:10.1126/scisignal.aat1082

Scalise, M., Pochini, L., Galluccio, M., and Indiveri, C. (2016). Glutamine transport. From energy supply to sensing and beyond. *Biochim. Biophys. acta* 1857 (8), 1147–1157. doi:10.1016/j.bbabio.2016.03.006

Scott, R. A., Lagou, V., Welch, R. P., Wheeler, E., Montasser, M. E., Luan, J., et al. (2012). Large-scale association analyses identify new loci influencing glycemic traits and

provide insight into the underlying biological pathways. *Nat. Genet.* 44 (9), 991–1005. doi:10.1038/ng.2385

Scuteri, A., Sanna, S., Chen, W. M., Uda, M., Albai, G., Strait, J., et al. (2007). Genome-wide association scan shows genetic variants in the FTO gene are associated with obesity-related traits. *PLoS Genet.* 3 (7), e115. doi:10.1371/journal.pgen.0030115

Seiler, S. E., Xu, D., Ho, J. P., Lo, K. A., Buehrer, B. M., Ludlow, Y. J., et al. (2015). Characterization of a primary Brown adipocyte culture system derived from human fetal interscapular fat. *Adipocyte* 4 (4), 303–310. doi:10.1080/21623945.2015.1042192

Sharp, L. Z., Shinoda, K., Ohno, H., Scheel, D. W., Tomoda, E., Ruiz, L., et al. (2012). Human BAT possesses molecular signatures that resemble beige/brite cells. *PLoS one* 7 (11), e49452. doi:10.1371/journal.pone.0049452

Shaw, A., Tóth, B. B., Király, R., Arianti, R., Csomós, I., Póliska, S., et al. (2021). Irisin stimulates the release of CXCL1 from differentiating human subcutaneous and deep-neck derived adipocytes via upregulation of NFκB pathway. *Front. Cell Dev. Biol.* 9, 737872. doi:10.3389/fcell.2021.737872

Shinoda, K., Luijten, I. H., Hasegawa, Y., Hong, H., Sonne, S. B., Kim, M., et al. (2015). Genetic and functional characterization of clonally derived adult human Brown adipocytes. *Nat. Med.* 21 (4), 389–394. doi:10.1038/nm.3819

Szatmári-Tóth, M., Shaw, A., Csomós, I., Mocsár, G., Fischer-Posovszky, P., Wabitsch, M., et al. (2020). Thermogenic activation downregulates high mitophagy rate in human masked and mature beige adipocytes. *Int. J. Mol. Sci.* 21 (18), 6640. doi:10.3390/ijms21186640

Tanaka, T., Ngwa, J. S., van Rooij, F. J., Zillikens, M. C., Wojczynski, M. K., Frazier-Wood, A. C., et al. (2013). Genome-wide meta-analysis of observational studies shows common genetic variants associated with macronutrient intake. *Am. J. Clin. Nutr.* 97 (6), 1395–1402. doi:10.3945/ajcn.112.052183

Tóth, B. B., Arianti, R., Shaw, A., Vámos, A., Veréb, Z., Póliska, S., et al. (2020). FTO intronic SNP strongly influences human neck adipocyte browning determined by tissue and PPARγ specific regulation: A transcriptome analysis. *Cells* 9 (4), 987. doi:10.3390/cells9040987

Townsend, K. L., and Tseng, Y. H. (2014). Brown fat fuel utilization and thermogenesis. *Trends Endocrinol. Metab.* 25 (4), 168–177. doi:10.1016/j.tem.2013.12.004

Vámos, A., Shaw, A., Varga, K., Csomós, I., Mocsár, G., Balajthy, Z., et al. (2022). Mitophagy mediates the beige to white transition of human primary subcutaneous adipocytes *ex vivo*. *Pharm. (Basel, Switz.)* 15 (3), 363. doi:10.3390/ph15030363

Virtanen, K. A., Lidell, M. E., Orava, J., Heglind, M., Westergren, R., Niemi, T., et al. (2009). Functional Brown adipose tissue in healthy adults. *N. Engl. J. Med.* 360 (15), 1518–1525. doi:10.1056/NEJMoa0808949

Wajchenberg, B. L. (2000). Subcutaneous and visceral adipose tissue: Their relation to the metabolic syndrome. *Endocr. Rev.* 21 (6), 697–738. doi:10.1210/edrv.21.6.0415

Wang, K., Li, W. D., Zhang, C. K., Wang, Z., Glessner, J. T., Grant, S. F., et al. (2011). A genome-wide association study on obesity and obesity-related traits. *PLoS one* 6 (4), e18939. doi:10.1371/journal.pone.0018939

Wang, L., Yu, Q., Xiong, Y., Liu, L., Zhang, X., Zhang, Z., et al. (2013). Variant rs1421085 in the FTO gene contribute childhood obesity in Chinese children aged 3-6 years. *Obes. Res. Clin. Pract.* 7 (1), e14–e22. doi:10.1016/j.orcp.2011.12.007

Wang, S., Lin, Y., Gao, L., Yang, Z., Lin, J., Ren, S., et al. (2022). PPAR-γ integrates obesity and adipocyte clock through epigenetic regulation of Bmal1. *Theranostics* 12 (4), 1589–1606. doi:10.7150/thno.69054

Wheeler, E., Huang, N., Bochukova, E. G., Keogh, J. M., Lindsay, S., Garg, S., et al. (2013). Genome-wide SNP and CNV analysis identifies common and low-frequency variants associated with severe early-onset obesity. *Nat. Genet.* 45 (5), 513–517. doi:10.1038/ng.2607

Wolins, N. E., Quaynor, B. K., Skinner, J. R., Tzekov, A., Croce, M. A., Gropler, M. C., et al. (2006). OXPAT/PAT-1 is a PPAR-induced lipid droplet protein that promotes fatty acid utilization. *Diabetes* 55 (12), 3418–3428. doi:10.2337/db06-0399

Wu, J., Boström, P., Sparks, L. M., Ye, L., Choi, J. H., Giang, A. H., et al. (2012). Beige adipocytes are a distinct type of thermogenic fat cell in mouse and human. *Cell* 150 (2), 366–376. doi:10.1016/j.cell.2012.05.016

Wu, Q., Ortegon, A. M., Tsang, B., Doege, H., Feingold, K. R., and Stahl, A. (2006). FATP1 is an insulin-sensitive fatty acid transporter involved in diet-induced obesity. *Mol. Cell. Biol.* 26 (9), 3455–3467. doi:10.1128/MCB.26.9.3455-3467.2006

Yoneshiro, T., Wang, Q., Tajima, K., Matsushita, M., Maki, H., Igarashi, K., et al. (2019). BCAA catabolism in Brown fat controls energy homeostasis through SLC25A44. *Nature* 572 (7771), 614–619. doi:10.1038/s41586-019-1503-x

Zeng, X., Ye, M., Resch, J. M., Jedrychowski, M. P., Hu, B., Lowell, B. B., et al. (2019). Innervation of thermogenic adipose tissue via a calsyntenin 3β-S100b axis. *Nature* 569 (7755), 229–235. doi:10.1038/s41586-019-1156-9

Zou, Y., Lu, P., Shi, J., Liu, W., Yang, M., Zhao, S., et al. (2017). IRX3 promotes the browning of white adipocytes and its rare variants are associated with human obesity risk. *EBioMedicine* 24, 64–75. doi:10.1016/j.ebiom.2017.09.010